Molecular Pharmacology Fast Forward. Published on March 20, 2012 as doi: 10.1124/mol.111.077446
This article has not been copyedited and formatted. The final version may differ from this version.

Title Page

Identification and Characterization of a Novel Class of c-Jun N-terminal Kinase Inhibitors

Igor A. Schepetkin, Liliya N. Kirpotina, Andrei I. Khlebnikov, Tracey S. Hanks, Irina Kochetkova, David W. Pascual, Mark A. Jutila, and Mark T. Quinn

Department of Immunology and Infectious Diseases, Montana State University, Bozeman, MT, USA (I.A.S., L.N.K., T.S.H., I.K., D.W.P., M.A.J., and M.T.Q.) and *Department of Chemistry, Altai State Technical University, Barnaul, Russia (A.I.K.)*

Molecular Pharmacology Fast Forward. Published on March 20, 2012 as DOI: 10.1124/mol.111.077446
This article has not been copyedited and formatted. The final version may differ from this version.

Running Title Page

Running title: Novel Class of c-Jun N-terminal Kinase Inhibitors

Address for Correspondence: Dr. Mark T. Quinn
Immunology and Infectious Diseases
Montana State University
Bozeman, MT 59717
Phone: 406-994-4707; Fax 406-994-4303
E-mail: mquinn@montana.edu

Number of text pages: 26

Number of tables: 5

Number of figures: 8

Number of references: 78

Number of words in Abstract: 243

Number of words in Introduction: 593

Number of words in Discussion: 941

Abbreviations

AP-1, activating protein 1; CK1δ, casein kinase 1δ; DMSO, dimethyl sulfoxide; DTH, delayed-type hypersensitivity; IL, interleukin; FBS, fetal bovine serum; GAPDH, glyceraldehyde 3-phosphate dehydrogenase, GM-CSF, granulocyte-macrophage colony-stimulating factor; IFN, interferon; JNK, c-Jun N-terminal kinase; LPS, lipopolysaccharide; MAPK, mitogen activated protein kinase; NF-κB, nuclear factor-κB; NO, nitric oxide; OVA, ovalbumin; PBMC, peripheral blood mononuclear cell; PI3K, phosphoinositide 3-kinase; SAR, structure-activity relationship; AS252424, TNF, tumor necrosis factor; 5-[[5-(4-fluoro-2-hydroxyphenyl)-2-furanyl]methylene]-2,4-thiazolidinedione; AS 605240, 5-(6-quinoxalinylmethylene)-2,4-thiazolidine-2,4-dione; PF670462, 4-[1-cyclohexyl-4-(4-fluorophenyl)-1*H*-imidazol-5-yl]-2-pyrimidinamine dihydrochloride; SP600125, anthra[1-9-*cd*]pyrazol-6(2*H*)-one; TCS PIM-1 1, 3-cyano-4-phenyl-6-(3-bromo-6-hydroxy)phenyl-2(1*H*)-pyridone

Molecular Pharmacology Fast Forward. Published on March 20, 2012 as DOI: 10.1124/mol.111.077446
This article has not been copyedited and formatted. The final version may differ from this version.

Abstract

In efforts to identify novel small molecules with anti-inflammatory properties, we discovered a unique series of tetracyclic indenoquinoxaline derivatives that inhibited lipopolysaccharide (LPS)-induced NF-κB/AP-1 activation. Compound **IQ-1** (11*H*-indeno[1,2-b]quinoxalin-11-one oxime) was found to be a potent, non-cytotoxic inhibitor of pro-inflammatory cytokine [interleukin (IL)-1α, IL-1β, IL-6, IL-10, tumor necrosis factor (TNF)-α, interferon (IFN)-γ, and granulocyte-macrophage colony-stimulating factor (GM-CSF)] and nitric oxide production by human and murine monocyte/macrophages. Three additional potent inhibitors of cytokine production were identified through further screening of **IQ-1** analogs. The sodium salt of **IQ-1** inhibited LPS-induced TNF-α and IL-6 production in MonoMac-6 cells with IC_{50} values of 0.25 and 0.61 μM, respectively. Screening of 131 protein kinases revealed that derivative **IQ-3** (11*H*-indeno[1,2-b]quinoxalin-11-one-O-(2-furoyl)oxime) was a specific inhibitor of the c-Jun N-terminal kinase (JNK) family, with preference for JNK3. This compound, as well as **IQ-1** and three additional oxime indenoquinoxalines, were found to be high-affinity JNK inhibitors with nanomolar binding affinity and ability to inhibit c-Jun phosphorylation. Furthermore, docking studies showed that hydrogen bonding interactions of the active indenoquinoxalines with Asn152, Gln155, and Met149 of JNK3 played an important role in enzyme binding activity. Finally, we showed that the sodium salt of **IQ-1** had favorable pharmacokinetics and inhibited the ovalbumin-induced $CD4^+$ T-cell immune response in a murine delayed-type hypersensitivity (DTH) model *in vivo*. We conclude that compounds with an indenoquinoxaline nucleus can serve as specific small-molecule modulators for mechanistic studies of JNKs, as well as a potential leads for the development of anti-inflammatory drugs.

Molecular Pharmacology Fast Forward. Published on March 20, 2012 as DOI: 10.1124/mol.111.077446
This article has not been copyedited and formatted. The final version may differ from this version.

Introduction

Members of activating protein 1 (AP-1) and nuclear factor-κB (NF-κB) families of transcription factors control many essential physiological and pathological processes including inflammation, immune responses, host-defense, and cancer [reviewed in (Peng, 2008;Ghosh and Hayden, 2008;Vaiopoulos et al., 2010)]. Because these transcription factors are key regulators of the inducible expression of many pro-inflammatory mediators, their inhibition by small-molecule compounds represents an area of interest for new drug development. Chemical inhibitors of AP-1 and NF-κB reported so far include compounds that block activation of these transcription factors, nuclear translocation of activated NF-κB/AP-1, and their DNA binding (Watanabe et al., 2008;Ghosh and Hayden, 2008;Kang et al., 2009;Oh et al., 2010;Law et al., 2010). Most signaling pathways upstream of NF-κB/AP-1 activation converge on level of three mitogen activated protein kinase (MAPK) families, which include extracellular signal-regulated protein kinases (ERKs), p38, and c-Jun N-terminal kinases (JNKs) [reviewed in (Bhagwat, 2007)].

JNKs are directly involved in controlling regulation of AP-1 transcriptional activity and, for this reason, drug discovery efforts have focused on the development of JNK inhibitors for treatment of chronic inflammatory diseases (Bennett et al., 2003;Wagner and Laufer, 2006;Jung et al., 2010). One of the targets of activated JNKs is c-Jun, which is specifically phosphorylated on Ser63 and/or Ser73, making this protein capable of binding AP-1 sites in the nucleus (Hibi et al., 1993). JNKs also phosphorylate other AP-1 proteins, including JunB, JunD, and ATF2 [reviewed in (Davis, 2000)]. Although AP-1 and NF-κB are regulated by different signaling pathways, cross-talk between these pathways occurs, mediated in part by the ability of certain Jun and Fos family proteins to interact with the p65 subunit of NF-κB (Fujioka et al., 2004).

Molecular Pharmacology Fast Forward. Published on March 20, 2012 as DOI: 10.1124/mol.111.077446
This article has not been copyedited and formatted. The final version may differ from this version.

Development of inhibitors specific for the JNK family has gained increasing interest in recent years, and several novel small molecule JNK inhibitors have been described (Bennett et al., 2001;Gaillard et al., 2005;Szczepankiewicz et al., 2006;Shin et al., 2009;Kamenecka et al., 2009;Christopher et al., 2009;He et al., 2011;Plantevin Krenitsky et al., 2012). These inhibitors demonstrated anti-inflammatory and neuroprotective activities (Bennett et al., 2001;Carboni et al., 2004;Gaillard et al., 2005;Nijboer et al., 2010;Chambers et al., 2011;Plantevin Krenitsky et al., 2012). Although the anti-inflammatory effects of JNK inhibitors may involve AP-1 and NF-κB transcription pathways, their neuroprotective action probably also depends on inhibition of JNK-dependent activation of proapoptotic signals (Yeste-Velasco et al., 2009).

The mechanisms of JNK signaling leading to NF-κB/AP-1 activation are complex and not completely defined, thus cell-based strategies for chemical library screening have been suggested as the most reasonable option for studying these pathways [e.g., (Kang et al., 2009;Peddibhotla et al., 2010)]. In addition, cell-based screening can help to predict compound bioavailability and toxicity and facilitate the rapid identification of compounds inducing complex cellular responses. In the present study, we screened a library of 10,000 small-molecule compounds for their ability to inhibit lipopolysaccharide (LPS)-induced NF-κB/AP-1 reporter activity in a cell-based assay and identified a novel synthetic compound, 11*H*-indeno[1,2-b]quinoxalin-11-one oxime, designated as **IQ-1**. Further studies showed that this compound and several related analogs inhibited the production of pro-inflammatory cytokines and nitric oxide (NO) by LPS-stimulated monocytes/macrophages and peripheral blood mononuclear cells (PBMCs). Nine additional inhibitors of cytokine [interleukin (IL)-6 and tumor necrosis factor-α (TNF-α)] production were identified through further screening of **IQ-1** analogs. Kinase profiling of 131 different protein kinases showed one of the most potent indenoquinoxaline analogs, **IQ-3**, was a specific JNK inhibitor. Indeed, **IQ-3** and the other oxime-derived indenoquinoxalines

Molecular Pharmacology Fast Forward. Published on March 20, 2012 as DOI: 10.1124/mol.111.077446
This article has not been copyedited and formatted. The final version may differ from this version.

were found to be high-affinity JNK inhibitors exhibiting nanomolar binding affinity. Finally, the sodium salt of **IQ-1** demonstrated favorable pharmacokinetics and inhibited ovalbumin-induced CD4+ T-cell immune responses *in vivo*.

Molecular Pharmacology Fast Forward. Published on March 20, 2012 as DOI: 10.1124/mol.111.077446
This article has not been copyedited and formatted. The final version may differ from this version.

Materials and Methods

Materials. Dimethyl sulfoxide (DMSO), LPS from *Escherichia coli* K-235, and Histopaque 1077 were purchased from Sigma Chemical Co. (St. Louis, MO). The chemical diversity set of 10,000 compounds was obtained from TimTec Inc. (Newark, DE). Compounds **IQ-3** through **IQ-18** were purchased from TimTec Inc., Scientific Exchange (Center Ossipee, NH), ChemBridge (San Diego, CA), Specs (Delft, The Netherlands), InterBioScreen (Moscow, Russia), and Vitas-M (Moscow, Russia). The compounds were diluted in DMSO at a concentration of 2 mg/ml and stored at –80°C. Kinase inhibitors PF670462, AS252424, AS605240, TCSPIM-1 1, and SP600125 were from Tocris Bioscience (Ellisville, MO).

Synthesis of IQ-1 Sodium Salt (IQ-1S). IQ-1S was synthesized, as described previously (Pearson, 1962;Obot and Obi-Egbedi, 2010). The structure of the oxime was supported by NMR and mass-spectroscopy. ^{1}H NMR (500 MHz, DMSO-d_6), ppm: 7.57 (1H, *t*, *J* 7.5 Hz, H-2), 7.62 (1H, *t*, *J* 7.5 Hz, H-3), 7.76 (2H, *m*, H-7 and H-8), 8.13 (2H, *m*, H-6 and H-9), 8.21 (1H, *d*, *J* 7.5 Hz, H-4), 8.79 (1H, *d*, *J* 7.5 Hz, H-1). MS (ESI) m/z 270.06 [M+H^{+}].

Cell Culture. All cells were cultured at 37°C in a humidified atmosphere containing 5% CO_2. THP-1Blue cells obtained from InvivoGen were cultured in RPMI 1640 medium (Mediatech Inc., Herndon, VA) supplemented with 10% (v/v) fetal bovine serum (FBS), 100 µg/ml streptomycin, 100 U/ml penicillin, 100 µg/ml zeocin, and 10 µg/ml blasticidin S. Human monocyte-macrophage MonoMac-6 cells (DSMZ; Brunswick, Germany) were grown in RPMI 1640 (Mediatech Inc.; Herndon, VA) supplemented with 10% (v/v) FBS, 10 µg/mL bovine insulin, 100 µg/mL streptomycin, and 100 U/mL penicillin. The mouse macrophage cell line J774.A1 was grown in DMEM without phenol red and supplemented with 3% (v/v) bovine serum, 100 µg/ml streptomycin, and 100 U/ml penicillin. Cells were grown to confluence in sterile tissue culture flasks and gently detached by scraping.

Molecular Pharmacology Fast Forward. Published on March 20, 2012 as DOI: 10.1124/mol.111.077446
This article has not been copyedited and formatted. The final version may differ from this version.

Isolation of human PBMCs. Blood was collected from healthy donors in accordance with a protocol approved by the Institutional Review Board at Montana State University. PBMCs were isolated from blood using dextran sedimentation and Histopaque 1077 gradient separation, as described previously (Schepetkin et al., 2009).

Library Screening. We screened the 10,000-compound chemical diversity set for inhibitory of NF-κB/AP-1 reporter activity in THP-1Blue cells. Human monocytic THP-1Blue cells are stably transfected with a secreted embryonic alkaline phosphatase gene that is under the control of a promoter inducible by NF-κB/AP-1. THP-1Blue cells (2 x 10^5 cells/well) were pretreated with 20 μg/ml of test compound or DMSO for 30 min, followed by addition of 200 ng/ml LPS or buffer for 24 h, and alkaline phosphatase activity was measured in cell supernatants using QUANTI-Blue mix (InvivoGen). For selected lead compounds, the concentrations of inhibitor that caused 50% inhibition of the NF-κB reporter activity (IC_{50}) were calculated by plotting percent inhibition against the logarithm of inhibitor concentration (at least 5 points).

Cytokine Analysis. Human PBMCs were plated in 96-well plates at a density of 2 x 10^5 cells/well in culture medium supplemented with 3% (v/v) endotoxin-free FBS. PBMCs were pretreated with 20 μM of compound **IQ-1** or DMSO for 30 min, followed by addition of 200 ng/ml LPS for 24 h. A human cytokine MultiAnalyte ELISArray Kit from SABiosciences (Frederick, MD) was used to evaluate various cytokines (IL-1α, IL-1β, IL-2, IL-4, IL-6, IL-8, IL-10, IL-12, IL-17A, interferon (IFN)-γ, TNF-α, and granulocyte-macrophage colony-stimulating factor (GM-CSF) in supernatants of PBMCs.

Human TNF-α and IL-6 ELISA kits (BD Biosciences) were used to confirm the inhibitory effect of selected compounds on TNF-α or IL-6 production. Human PBMCs or MonoMac-6 cells were plated in 96-well plates at a density of 2 x 10^5 cells/well in culture

Molecular Pharmacology Fast Forward. Published on March 20, 2012 as DOI: 10.1124/mol.111.077446
This article has not been copyedited and formatted. The final version may differ from this version.

medium supplemented with 3% (v/v) endotoxin-free FBS. Cells were pretreated with test compound or DMSO for 30 min, followed by addition of 200 ng/ml LPS for 24 h. For selected compounds, the concentration of inhibitor that caused 50% inhibition of the cytokine production (IC_{50}) was calculated by plotting percent inhibition against the logarithm of inhibitor concentration (at least 5 points).

Determination of Nitric Oxide (NO). J774.A1 macrophage cells were plated at a density of 1.5 x 10^6 cells/ml in 96-well flat-bottomed tissue culture plates in culture medium without phenol red and supplemented with 3% (v/v) bovine serum. The cells were pretreated with different concentrations of tested compounds or DMSO for 30 min, followed by addition of 200 ng/ml LPS for 24 h. At the end of the culture period, supernatants (100 µl) were removed and assayed for NO. Nitrite ion (NO_2^-) concentration was used as an indication of NO production, and the amount of NO_2^- in the culture medium was determined according to the colorimetric method using $NaNO_2$ as a standard. Briefly, 100 µl of cell culture supernatant were mixed with an equal volume of Griess reagent [0.1% (w/v) *N*-(1-naphthyl)ethylenediamine dihydrochloride and 1% (w/v) sulfanilamide in 5% (v/v) phosphoric acid]. The samples were incubated at room temperature for 20 min, and absorbance was measured at 540 nm using a SpectraMax Plus microplate reader. The concentration of inhibitor that caused 50% inhibition of the NO production (IC_{50}) was calculated by plotting percent inhibition against the logarithm of inhibitor concentration (at least 5 points).

Cytotoxicity Assay. Cytotoxicity was analyzed with a CellTiter-Glo Luminescent Cell Viability Assay Kit from Promega (Madison, WI), according to the manufacturer's protocol. Cells were treated with compound under investigation and cultivated for 24 h. Following treatment, the cells were allowed to equilibrate to room temperature for 30 min, substrate was added, and the samples were analyzed with a Fluoroscan Ascent FL. The concentration of

Molecular Pharmacology Fast Forward. Published on March 20, 2012 as DOI: 10.1124/mol.111.077446
This article has not been copyedited and formatted. The final version may differ from this version.

inhibitor that caused 50% cell amount during 24 h-incubation (via toxicity of inhibition of cell growing) (IC_{50}) was calculated by plotting percent inhibition against the logarithm of inhibitor concentration (at least 5 points).

Kinase Profiling and K_d Determination. Kinase profiling was performed by KINOMEscan (DiscoveRx, San Diego, CA) using a panel of 91 protein kinases, as described previously (Fabian et al., 2005;Karaman et al., 2008) and by Luceome Biotechnologies (Tucson, AZ) using a panel of 60 protein kinases, as described by Jester et al. (Jester (Jester et al., 2010). Briefly, kinases were produced and displayed on T7 phage or expressed in HEK-293 cells. Binding reactions were performed at room temperature for one hr, and the fraction of kinase not bound to test compound was determined by capture with an immobilized affinity ligand and quantified by quantitative PCR. Primary screening at fixed concentrations of compounds was performed in duplicate. Selected hit compounds were submitted for dissociation constant (K_d) determination using the same platform. For dissociation constant K_d determination, a 12-point half-log dilution series (a maximum concentration of 100 μM) was used. Assays were performed in duplicate, and their mean value is displayed.

JNK3 Enzyme Kinetic Assay. JNK3 enzymatic activity was determined by measuring the phosphorylation of glutathione S-transferase tagged activating transcription factor 2 (GST-ATF2) by Reaction Biology Corporation (Malvern, PA). Briefly, the enzyme reactions were conducted in buffer containing 25 mM Hepes at pH 7.5, 2 mM dithiothreitol, 10 mM $MgCl_2$, 1 mM EGTA, 0.02% Brij35, 0.01 mM Na_3VO_4, 0.02 mg/ml BSA, and 1% DMSO. These assays contained 25 nM recombinant human full length JNK3 (GST-tagged; M_r 76.6. kDa), 5 μM recombinant human GST-ATF2 (a.a. 19-96; M_r 36.7 kDa), nonradioactive ATP (10−100 μM), and [γ-^{33}P] ATP. **IQ-3** was added to the mixture using acoustic technology and incubated for 20 min to ensure the compound was equilibrated and bound to the enzyme. Different

Molecular Pharmacology Fast Forward. Published on March 20, 2012 as DOI: 10.1124/mol.111.077446
This article has not been copyedited and formatted. The final version may differ from this version.

concentrations of ATP were added to initiate the reaction, and the activity was monitored every 5-15 min.

Western Blotting. MonoMac-6 monocytic cells were pretreated with different concentrations of the compounds under investigation for 30 min and treated with LPS (200 ng/ml) or vehicle for another 30 min. Cells were washed twice with Hank's balanced Salt solution, and cell lysates were prepared using lysis buffer from the JNK kinase assay kit (Cell Signaling Technology, Danvers, MA). Cell lysates (from 5 x 10^6 cells) were separated on 10% SDS polyacrylamide gels, transferred to nitrocellulose membranes, and the blots were probed with antibodies against c-Jun, phospho-c-Jun (S63), and glyceraldehyde 3-phosphate dehydrogenase (GAPDH) (Cell Signaling Technology, Danvers, MA), followed by horseradish peroxidase-conjugated secondary antibody (Thermo Fisher Scientific, Rockford, IL). The blots were developed using SuperSignal West Femto chemiluminescent substrate (Thermo Fisher Scientific) and visualized with a FluorChem FC2 imaging system (Alpha Innotech Corporation, San Leandro, CA). Quantitation of the chemiluminescent signal was carried out using AlfaView software version 3.0.0.0.

Compound Stability and Pharmacokinetic Analysis. For *ex vivo* analysis of **IQ-1S** stability, **IQ-1S** was incubated in mouse serum at final concentration 50 μM for 2, 30, 60, 120, 210, 300, and 600 min at room temperature. Serum sample aliquots (110 μL) were mixed with 130 μL of acetonitrile to precipitate proteins, centrifuged at 8,000 *g* for 5 min, and the supernatants were filtrated using a 0.45 μm filter. Filtered samples were analyzed by reverse phase HPLC using a Phenomenex Jupiter C18 300A column (5 μm, 25 cm × 0.46 cm) at 40°C with a mobile phase of 40:60 v/v acetonitrile:water containing 0.1% (v/v) TFA and a flow rate of 1.0 ml/min. The elution was monitored at 290 nm, the wavelength corresponding to λ_{max} for **IQ-1S**. For *in vivo* analysis, 12.5 or 30 mg/kg doses of **IQ-1S** were administered *i.p.* to BALB/c

Molecular Pharmacology Fast Forward. Published on March 20, 2012 as DOI: 10.1124/mol.111.077446
This article has not been copyedited and formatted. The final version may differ from this version.

mice (15-20 animals/group), and the mice were sacrificed at various time points following compound administration. For quantification, a calibration curve was established using mouse serum samples spiked with known concentrations of **IQ-1S** (0.1–20 μM), and a linear dependence of the peak area with **IQ-1S** concentration was obtained (correlation coefficient r=0.997). The area under the serum concentration-time curve ($AUC_{0\text{-}12h}$) was calculated using the linear trapezoidal method up to the last measured concentration.

Ovalbumin (OVA)-Specific Delayed-Type Hypersensitivity. $CD4^+$ T cells were purified using Dynal Mouse CD4 Negative Isolation kit (Invitrogen) from DO11.10 mouse spleens and lymph nodes (LNs). Purified $CD4^+$ T (3×10^6) cells were adoptively transferred to age- and sex- matched BALB/c mice (day 0). On day 1, all recipients were challenged with 100 μg OVA in incomplete Freund's adjuvant s.c. and treated i.p. with JNK inhibitor (12.5 mg/kg) in 0.125% DMSO or vehicle. Mice were treated repeatedly (i.p.) every 12 h for 5 total injections, and a delayed-type hypersensitivity (DTH) test was performed on day 5, as previously described (Kochetkova et al., 2010). The DTH response was monitored as the difference in ear swelling between OVA- and PBS-challenged pinna (the outer part of the ear).

Molecular Docking Analysis. Geometry of JNK3 was obtained by downloading a crystal structure of JNK3 complexed with JNK inhibitor SP600125 (Xie et al., 1998) from the Protein Data Bank (PDB, entry code 1PMV) into Molegro software. All solvent molecules were removed. Side chains of 39 residues (Lys68, Ile70, Gly71, Ser72, Gly73, Gln75, Gly76, Val78, Ala80, Val90, Ala91, Ile92, Lys93, Lys94, Met115, Ile124, Ser125, Leu126, Leu127, Tyr143, Leu144, Val145, Met146, Glu147, Leu148, Met149, Asp150, Ala151, Asn152, Cys154, Gln155, Ser193, Asn194, Val196, Val197, Lys198, Lys204, Leu206, Asp207) closest to the active ligand SP600125 were considered to be flexible in the docking procedure. These residues were identified using default option of “Setup Sidechain Flexibility” in Molegro, and a softening

parameter of 0.7 was applied during flexible docking, according to the standard protocol using the Molegro Virtual Docker (MVD) program (MVD 2010.4.2, Molegro ApS). It should be noted that the 39 residues assumed as flexible almost completely included 22 amino acids (Ile70, Gly71, Ser72, Gly73, Gln75, Gly76, Val78, Ala91, Lys93, Ile124, Met146, Glu147, Leu148, Met149, Asp150, Ala151, Asn152, Gln155, Ser193, Asn194, Val196, and Leu206), which are considered as belonging to the JNK3 ATP-binding pocket (Xie et al., 2008). Search space was set as a sphere having 11 Å radius and positioned at the gravity center of all heavy atoms of co-crystallized ligand SP600125. This search space included all of the flexible residues mentioned above. The docking methodology was verified by the location of the redocked X-ray ligand (SP600125). The alignment of best predicted conformation of SP600125 yielded RMS deviation of 1.02 Å, indicating that the docking simulation was able to reproduce the X-ray structure.

Before docking, structures of compounds were pre-optimized by HyperChem software with the MM+ force field and saved in Tripos MOL2 format. The JNK3 macromolecule and all the ligand structures were imported into MVD. The options “Create explicit hydrogens,” “Assign charges (calculated by MVD),” and “Detect flexible torsions in ligands” were enabled during importing. Appropriate protonation states of ligands were also automatically generated at this step.

Molecular Pharmacology Fast Forward. Published on March 20, 2012 as DOI: 10.1124/mol.111.077446
This article has not been copyedited and formatted. The final version may differ from this version.

Results

Primary High-Throughput Screening and Hit Validation

To identify novel compounds that inhibited LPS-induced activation of NF-κB/AP-1 in macrophages, we screened a chemical diversity library of 10,000 drug-like compounds with molecular weights from 200 to 550 Da. This library of commonly accepted pharmaceutical hit structures was randomly assembled to maximize chemical diversity.

A compound was defined as a hit if it exhibited >50% inhibition of LPS-induced NF-κB/AP-1 reporter activity in human monocytic THP-1Blue cells at a final compound concentration of 20 μg/mL. From the primary screening, 48 inhibitory compounds were selected (0.48% hit rate). The size of the hit set was further reduced by applying a series of experimental filters, including a determination of the dose–response relationship for inhibition of reporter activity. A compound was determined as desirable if it had IC_{50} <20 μM and was non-toxic at concentrations <40 μM. Only one compound, indenoquinoxaline 1 (designated as **IQ-1**), met these conditions and was selected as a prospective inhibitor of NF-κB/AP-1 activity with an IC_{50} of 2.3 ± 0.41 μM. The structure of **IQ-1** and a representative inhibitory activity curve are shown in **Figure 1**. A cytotoxicity assay ruled out the possibility that repressed reporter activity was a consequence of possible cell death (**Figure 1**). Additionally, **IQ-1** did not affect alkaline phosphatase activity directly (data not shown). Note that this library was previously screened for different biological activities, resulting in selection of hit compounds that inhibited target enzymes (Schepetkin et al., 2006;Schepetkin et al., 2007a), activated the phagocyte NADPH-oxidase (Schepetkin et al., 2007b), and stimulated *N*-formyl-peptide receptors (Schepetkin et al., 2007b;Kirpotina et al., 2010), supporting the specificity of our screening in the present study.

We next evaluated the effect of **IQ-1** on LPS-induced cytokine production in human PBMCs. Among the twelve cytokines analyzed, LPS (200 ng/mL) consistently induced five (IL-

Molecular Pharmacology Fast Forward. Published on March 20, 2012 as DOI: 10.1124/mol.111.077446
This article has not been copyedited and formatted. The final version may differ from this version.

1α, IL-1β, IL-6, IL-10, and TNF-α) in PBMCs, as compared with DMSO-treated control cells. Production of all of these cytokines was significantly inhibited by 20 μM **IQ-1** (**Figure 2**). Among of them, TNF-α production was inhibited completely by **IQ-1** (>99%), the levels of IL-1α, IL-1β, and IL-10 were decreased by 85%, and IL-6 production was decreased by 33%. IL-8 production was inconclusive because of high background production by PBMCs, a problem which has also been documented previously [e.g. (Kikkert et al., 2008;Schepetkin et al., 2009)].

Secondary Screening and Structure–Activity Relationship (SAR) Analysis

Based on structure of **IQ-1**, 26 additional analogs were selected. In addition, the sodium salt of **IQ-1** (designated **IQ-1S**) was synthesized (see *Materials and Methods*). Compounds were evaluated for inhibition of LPS-induced NF-κB/AP-1 reporter activity in monocytic THP-1Blue cells, and the structures and biological activities of the analogs are shown in **Table 1**. Ten of these compounds were found to have inhibitory activity with IC_{50} values <7 μM. Additionally, all of the active compounds were non-toxic in THP1-Blue cells at concentrations <40 μM (**Table 1**).

The selected inhibitors contained oxime (**IQ-1** and **IQ-1S**), *O*-acyl-oxime (**IQ-2** through **IQ-6**), unsubstituted hydrazone (**IQ-7**), (thio)semicarbazone (**IQ-8** and **IQ-9**), or acylhydrazone (**IQ-10**) functions. Inspection of the inactive derivatives (**IQ-11** through **IQ-16**) suggested an overall trend of decreased activity with increased bulkiness of R for compounds with an acylhydrazone moiety (**Table 1**). Other inactive compounds were characterized by N-phenyl-imine (**IQ-17** and **IQ-19**), 3,4-dimethoxyphenyl imine (**IQ-20**), and carbonyl (**IQ-18**, **IQ-22** through **IQ-26**) groups as R/R_1 substituents (**Table 1** and **Supplemental Table S1**). Compounds **IQ-19** through **IQ-26** also contain additional heterocyclic moiety substituents (**Supplemental Table S1**). Thus, within this series of polycyclic analogs, the nature of the side chain oxime or

Molecular Pharmacology Fast Forward. Published on March 20, 2012 as DOI: 10.1124/mol.111.077446
This article has not been copyedited and formatted. The final version may differ from this version.

(acyl)hydrazone R substituent was found to be critical for biological activity. It should be noted that the inactive compounds were more lipophilic (mean LogP = 3.90) than the active compounds (mean LogP = 2.89, with LogP <3.0 for 64% of the active compounds). In addition, three of the inactive compounds (**IQ-12**, **IQ-19**, and **IQ-20**) had lipophilic descriptors greater than the range of Lipinski's rule (i.e., LogP≤5) (**Supplemental Figure S1**). Although very high lipophilicity values lead to slow cell accumulation kinetics (Kornhuber et al., 2011), various other molecular descriptors also contribute to cell bioavailability and intercellular activity (see below).

Effect of Indenoquinoxalines on Production of Pro-inflammatory Mediators

To ensure that the activity of hit compounds was not unique to the transfected cells, eleven active compounds (**IQ-1S** and **IQ-1** through **IQ-10**) were evaluated for their ability to inhibit LPS-induced production of TNF-α and IL-6 in human monocytic MonoMac-6 cells and human PBMCs. Seven of these compounds inhibited LPS-induced TNF-α and IL-6 production in both cell systems (**Table 2**). As an example, the dose–dependent effect of **IQ-1** and **IQ-3** on LPS-induced TNF-α production in human PBMCs is shown in **Figure 3**. We also evaluated three compounds that were inactive in the reporter gene assay (**IQ-13**, **IQ-15**, and **IQ-18**) for their effect on LPS-induced TNF-α and IL-6 production in these cell systems. Consistent with the reporter gene assay, these compounds also did not alter production of pro-inflammatory mediators in MonoMac-6 cells and PBMCs (**Table 2**), supporting the selectivity of our assays. Note, however, that the inhibitory activity of LPS-induced cell responses in non-transfected cells was not uniform for all inhibitors, and some inhibitors identified in the reporter cell assay did not inhibit cytokine production in either MonoMac-6 cells or PBMCs (see **Table 2**). Among these were hydrozones **IQ-9** and **IQ-10**, which may be unstable in aqueous media (Kalia and Raines,

Molecular Pharmacology Fast Forward. Published on March 20, 2012 as DOI: 10.1124/mol.111.077446
This article has not been copyedited and formatted. The final version may differ from this version.

2008) and also exhibited toxicity toward some of our cells (**Table 2**). Thus, these compounds were excluded from further analysis. The reasons for differences in activity of **IQ-5** and **IQ-6** among the different cell systems are not clear. While both have similar structures, **IQ-6** has an additional O-Me group in the *meta*-position of the methoxybenzoic acid tail. Thus, their different chemical structures may result in different physical properties that affect their activity in various cell types, which have different biological properties, such as membrane permeability, expression of P-glycoproteins, etc. Indeed, macrophage differentiation is known to affect the level of expression of protein transporters involved in movement of exogenous molecules (Skazik et al., 2008;Moreau et al., 2011). Hence, different compounds may be active in one cell line and less active or even inactive in another.

The binding of NF-κB/AP-1 to the promoter of target genes enhances the expression of inducible NO synthase [reviewed in (Atreya et al., 2008;Vallières and Du Souich, 2010)]. Thus, the effect of compounds on NO production was also evaluated in the functional assays. Among the selected compounds, only oximes **IQ-1** through **IQ-4** and **IQ-1S** inhibited NO production in murine J774-A.1 macrophages (**Table 2**). Although all compounds were not cytotoxic at concentrations <40 μM in THP1-Blue and MonoMac-6 monocytic cells, the compounds with an ureido-imine function (**IQ-8** and **IQ-9**) were cytotoxic in murine J774.A4 cells and human PBMCs, respectively (**Table 2**).

Kinase Inhibition Profile of IQ-3

Protein kinases play critical roles in up-regulation of NF-κB/AP-1 transcriptional activity. Thus, **IQ-3**, which demonstrated potent inhibitory activity in all cell-based assays without cell toxicity (**Table 2**), was profiled against a diverse panel of 131 kinases, representing all known kinase families. **IQ-3** was profiled in a competition binding assay for its ability to compete with

Molecular Pharmacology Fast Forward. Published on March 20, 2012 as DOI: 10.1124/mol.111.077446
This article has not been copyedited and formatted. The final version may differ from this version.

an active-site directed ligand for 91 different kinases (DiscoveRx KINOMEscan) and for its ability to inhibit kinase activity of 60 different kinases (Luceome Biotechnologies), including 20 kinases common to both panels. **IQ-3** was screened at 10 μM, and the kinases for which >90% inhibition of ligand binding and kinase activity was observed were designated as "kinase targets of the compound." Four such kinase targets were identified, including casein kinase 1δ (CK1δ, gene symbol CSNK1D), JNK1, JNK2, and JNK3 (**Figure 4**). Furthermore, >99% inhibition of ligand binding and kinase activity by **IQ-3** was observed for three kinases (JNK1, JNK2, and JNK3) among the 131 different kinases tested (**Figure 4**). Thus, **IQ-3** demonstrated a high specific inhibition of human JNK isoforms.

To further evaluate the relative specificity of **IQ-3**, we compared its biological activity to that of a commercially available JNK inhibitor, SP600125. As shown in **Table 3**, the IC_{50} value for SP600125 was close to that of **IQ-3** and our active indenoquinoxaline derivatives for inhibition of LPS-induced TNF-α secretion by Mono-Mac6 and PBMCs (compare with **Table 2**) and was similar to the previously reported inhibition of cytokine production by SP600125 in other cell cultures (Bennett et al., 2001). However, SP600125 is relatively non-specific, and 13 of 28 tested kinases were inhibited with similar or greater potency than the JNKs (Bain et al., 2003). Thus, we compared the selectivity of **IQ-3** and SP600125 using the KINOMEscan assay platform. A selectivity score, S(10), based on >90% inhibition of ligand binding at a single 10 μM screen concentration, was calculated by dividing the "kinase targets of the compound" with the "total number of non-mutated kinases" in the panel (Karaman et al., 2008). The published kinase profile of SP600125 (Fabian et al., 2005) was used for determination its S(10) value. We found that the S(10) for **IQ-3** was much lower (0.044 = 4/91) compared to the S(10) for SP600125 (0.328 = 39/119), indicating much higher target kinase selectivity for **IQ-3**.

Molecular Pharmacology Fast Forward. Published on March 20, 2012 as DOI: 10.1124/mol.111.077446
This article has not been copyedited and formatted. The final version may differ from this version.

We also evaluated for comparison additional inhibitors for kinase targets (other than JNK) that had were found to have moderate ligand binding activity in the KINOMEScan assay, including PF670462 (dual CK1ε/CK1δ inhibitor), AS252424 and AS605240 [phosphoinositide 3-kinase γ (PI3Kγ) inhibitors], and TCSPIM-1 1 (PIM-1 inhibitor). These inhibitors were evaluated for their effect on LPS-induced TNF-α production in MonoMac-6 and PBMCs. Although all four inhibitors were non-toxic at the concentrations tested in these cells, only the CK1ε/CK1δ inhibitor (PF670462) inhibited LPS-induced TNF-α production (**Table 3**). Note, however, that PF670462 has been reported to be a non-specific MAP kinase inhibitor and can also inhibit JNK (**Supplemental Table S2**) and p38 MAPK (Perez et al., 2011), both which regulate TNF-α production and other pro-inflammatory cytokines via AP-1 and NF-κB transcription pathways (Bhagwat, 2007). Thus, these data provide further evidence for the high degree of specificity and potency of **IQ-3** as a JNK inhibitor, and suggest the observed inhibition of pro-inflammatory cytokine production is due to JNK inhibition by this compound, rather than effects on other kinase pathways.

Kinase Binding and Biological Activity of Selected Indenoquinoxalines

The kinase binding activity of additional selected indenoquinoxalines was tested using six target kinases [JNK1, JNK2, JNK3, CK1δ, PI3Kγ (gene symbol PIK3CG), and MKNK2], which exhibited the highest binding activity for **IQ-3** in the primary kinase profiling (see **Figure 4**). All compounds that were inactive in the NF-κB/AP-1 reporter assay (compounds **IQ-11** through **IQ-18**) also exhibited no or low (<40%) inhibition of ligand binding for these six kinases (**Supplemental Table S3**). Conversely, most compounds that were active in cell-based assays (see **Tables 1-2**) had a relatively high binding activity (>60% inhibition of ligand binding) for JNKs, with a few exceptions (**Supplemental Table S3**). For example, compound

Molecular Pharmacology Fast Forward. Published on March 20, 2012 as DOI: 10.1124/mol.111.077446
This article has not been copyedited and formatted. The final version may differ from this version.

IQ-5 exhibited only moderate inhibition of ligand binding to JNKs. In addition, the hydrazone derivatives (**IQ-8** through **IQ-10**), which inhibited NF-κB/AP-1 reporter activity (**Table 1**), failed to inhibit ligand binding to the JNKs (see **Supplemental Table S2**). It should be noted that these hydrazones were also less active or non-active when tested for inhibition of LPS-induced IL-6 production in MonoMac-6 monocytic cells and human PBMCs and did not inhibit LPS-induced NO production in J774.A1 macrophages (**Table 2**).

The six oxime indenoquinoxalines that exhibited relatively high competition for JNK ligand binding in the primary screening (all oxime derivatives except **IQ-5**) were submitted for determination of their binding affinities (K_d) to selected kinases. Indenoquinoxalines **IQ-1** through **IQ-4**, **IQ-6**, and **IQ-1S** had K_d values in the nanomolar range for all three JNKs, although these compounds had higher affinity for JNK3 versus JNK1 and JNK2, as well as the other kinases tested (**Table 4**).

To confirm that the active indenoquinoxalines inhibited JNK activity in cells, MonoMac-6 monocytic cells were pretreated with the selected compounds, stimulated with LPS, and the level of phospho-c-Jun (S63) was determined. Compounds **IQ-1** through **IQ-4**, **IQ-1S**, and positive control SP600125 all inhibited the c-Jun phosphorylation (**Figure 5A**). A representative dose–response inhibition of c-Jun phosphorylation in MonoMac-6 cells by compounds **IQ-1** and **IQ-3** is shown in **Figure 5B**. It should be noted, that compound **IQ-18**, which did not inhibit LPS-induced reporter activity (**Table 1**) or cytokine production (**Table 2**), also failed to inhibit c-Jun phosphorylation (**Figure 5A**), again supporting the specificity of our active inhibitors.

Kinase Inhibition Profile of Related Oximes and Hydrazones and Molecular Docking

Because all active indenoquinoxalines contained different oxime tails or unsubstituted hydrazone group, ten compounds with the same side groups, but different nuclei were submitted

Molecular Pharmacology Fast Forward. Published on March 20, 2012 as DOI: 10.1124/mol.111.077446
This article has not been copyedited and formatted. The final version may differ from this version.

to KINOMEscan for evaluation of their ability to inhibit ligand binding to selected kinases. However, none of these compounds were found to be "hits," based on our requirements (>90% inhibition of ligand binding at concentration 10 μM) (**Supplemental Table S4**). Thus, although oxime side groups may contribute important interactions in the JNK binding site, the tetracyclic nucleus appears to be responsible for proper ligand positioning.

To investigate the impact of each substructure in a ligand binding, we used molecular docking. The indenoquinoxaline-derived JNK inhibitors and selected inactive compounds were subjected to molecular docking into the JNK3 ligand binding site. We used the structure of this kinase because the selected indenoquinoxalines had higher binding affinity for JNK3 compared to JNK1/JNK2 (see **Table 4** and **Supplemental Table S3**). Nevertheless, our pre-docking experiments showed that the active compounds were actually docked into the ATP-binding pocket, which exhibits a high degree of homology (>98%) among all three JNKs (Yan et al., 2011). **IQ-12** and **IQ-14** were not included in the docking study because their long side chains contain many rotatable bonds and hence have high conformational flexibility. In addition, **IQ-1S** was not docked because the position of Na^+ after dissociation in the binding site could not be defined unambiguously.

The best docking poses obtained for active JNK inhibitors (**IQ-1** through **IQ-4**, **IQ-7,** and SP600125) and non-active compounds (**IQ-8** through **IQ-11**, **IQ-13**, and **IQ-15** through **IQ-18**) showed that these molecules were oriented similarly within a narrow cleft in the ligand binding site. As examples, the docking poses of selected active (**IQ-1** through **IQ-4**) and non-active (**IQ-8** through **IQ-10** and **IQ-18)** compounds are shown in **Figure 6** and **Supplemental Figure S2**, respectively. The tetracyclic moieties of the molecules were approximately parallel to each other and inserted deeply into the cleft. However, analysis of H-bond energies formed by the docked molecules of both active and inactive compounds (**Table 5**) indicated that the potent JNK

Molecular Pharmacology Fast Forward. Published on March 20, 2012 as DOI: 10.1124/mol.111.077446
This article has not been copyedited and formatted. The final version may differ from this version.

inhibitors had much stronger H-bonding interactions with JNK3 than the inactive indenoquinoxalines. Indeed, for the eight active compounds, including known JNK inhibitor SP600125, we calculated an average value of 4.83±1.84 kcal/mol, while an average value of 1.59±1.18 kcal/mol was obtained for H-bond energies with the nine inactive compounds (mean±S.D.).

Comparison of the docking pose of the most active JNK inhibitor (**IQ-3**) to the docking poses of SP600125, inactive indenoquinoxaline **IQ-18** (**Figure 7**), and the published coordinates of ATP [(Xie et al., 2008); PDB entry code 1JNK] showed that the oxime moiety of **IQ-3** is positioned in a similar orientation as that of the ATP purine base, anchored deep in the ATP-binding site among Ile70, Gy71, Ser72, Gly73, Gln75, Val78, Lys93, Leu148, Met149, Asp150, Ala151, Asn152, Ser193, Asn194, Ile195, Val196, Leu206, and Asp207 (amino acids within 4 Å from the **IQ-3** pose are given). Furthermore, Lineweaver-Burk analysis demonstrated that **IQ-3** was indeed a competitive inhibitor for the ATP binding site of JNK3 (**Supplemental Figure S3**). Overall, compounds **IQ-3** and SP600125 seem to bind similarly to JNK3, and their R groups (acylhydrazone and carbonyl) coincide in the overlaid poses (**Figure 7A**). **IQ-3** is anchored within the binding site due to the formation of H-bonds of the NH_2 group in the Asn152 side chain with both nitrogen and oxygen atoms in the ligand oxime tail (**Table 5 and Figure 7A**). Energies of these bonds were 2.33 and 0.75 kcal/mol, respectively. A relatively weak H-bond (1.39 kcal/mol) was also formed between the protonated nitrogen in the heterocyclic moiety of **IQ-3** and the carbonyl side group of Gln155 (**Figure 7A**). Note that the tetracyclic fragment of **IQ-3** adopts an opposite orientation when compared to the docking pose of inactive **IQ-18** (**Figure 7B**), while planes of these tetracyclic moieties almost coincide within the binding site. According to our docking study, inactive ketone **IQ-18** forms a relatively weak H-bond (1.56 kcal/mol) with Met149.

Molecular Pharmacology Fast Forward. Published on March 20, 2012 as DOI: 10.1124/mol.111.077446
This article has not been copyedited and formatted. The final version may differ from this version.

Most indenoquinoxalines with high JNK-binding affinity were H-bonded with Asn152, Gln155, or Met149 (**Table 5**), and these interactions involved participation of atoms in the oxime or (acetyl)hydrazone substituents of the active indenoquinoxalines investigated. Inactive compounds did not form H-bonds with JNK3 (**IQ-16** and **IQ-17**) or formed H-bonds with other residues of the kinase. For example, some inactive indenoquinoxalines were H-bonded with Gln155 or Met149 through their heterocyclic moiety (**IQ-9** and **IQ-18**) or formed weak H-bonds with Asn152 (**IQ-10**).

Thus, molecular docking suggests that H-bonding interactions with participation of (substituted) oxime and (acetyl)hydrazone groups play an important role for JNK3 kinase inhibitory activity of compounds with an indenoquinoxaline scaffold. The high inhibitory activity of these compounds could be modulated by H-bonding interactions with key residues Asn152, Gln155, or Met149 when a ligand is anchored to JNK3. It should be noted that Asn152 and Gln155 are not conserved in other MAPKs, and hence this difference may contribute to the selectivity of our inhibitors for JNKs over other kinases.

Pharmacokinetic Analysis of IQ-1S and Effect on OVA-Specific CD4+ T-Cell Immunity

The stability of **IQ-1S** in mouse serum (*ex vivo*) and pharmacokinetic analysis were evaluated by HPLC. HPLC analysis of **IQ-1S**-spiked serum samples *ex vivo* showed that **IQ-1S** eluted with a retention time (R_t) of 8.52 min (**Supplemental Figure S4A**). Although control serum had a background peak at R_t=3.5 min, this peak was not close to that of **IQ-1S**, allowing us to monitored serum concentrations without background interference (**Supplemental Figure S4A**). *Ex vivo* analysis of **IQ-1S** showed that it was quite stable in mouse serum, with >99% of the parent compound still present after the 10 hr incubation period at 25^{o}C (monitored by HPLC at 1, 2, 3, 4, 5, and 10 hrs) (data not shown). Following *i.p.* administration of **IQ-1S**, a rapid rise

Molecular Pharmacology Fast Forward. Published on March 20, 2012 as DOI: 10.1124/mol.111.077446
This article has not been copyedited and formatted. The final version may differ from this version.

in the serum concentration of **IQ-1S** was observed, peaking at ~5 min (**Supplemental Figure S4B).** When mice were dosed *i.p*. with 12.5 and 30 mg/kg of **IQ-1S**, the serum exposure of the compound was also good, with $AUC_{0\text{-}12h}$ values of 2.9 and 7.4 μM×hr, respectively. Based on these data, the IC_{50} and K_d values for *in vitro* activity of **IQ-1S** (**Tables 1**, **2**, and **4**), and the published doses used for *in vivo* multiple-dose application of SP600125 [25-30 mg/kg, daily (Han et al., 2001;Zoukhri et al., 2006)], we split the total daily dose for SP600125 and **IQ-1S** into two doses of 12.5 mg/kg. Indeed, splitting the total daily dose has been reported to be more effective than the same dose given once daily (Albert et al., 2006).

JNK signaling pathways play an important role in T-cell activation and cell proliferation during inflammatory responses (Sabapathy et al., 1999;Bennett et al., 2001;Chialda et al., 2005;Melino et al., 2008). For example, JNK inhibitor SP600125 has been reported to inhibit activation and differentiation of primary human $CD4^+$ T cell cultures (Bennett et al., 2001), inhibit paw swelling in a mouse model of collagen induced adjuvant arthritis (Gaillard et al., 2005), and attenuate lung inflammation in an OVA-induced murine asthma model (Chialda et al., 2005). Thus, to evaluate the *in vivo* anti-inflammatory effect of our novel JNK inhibitors, we used a model of OVA-specific adoptive immunity. DO11.10 $CD4^+$ T cells were sorted and adoptively transferred to BALB/c mice, which were then challenged with OVA and subsequently treated with JNK inhibitors or vehicle. Measurement of the DTH response revealed a significant suppression of OVA-induced ear swelling by SP600125 and **IQ-1S** relative to vehicle treated mice (**Figure 8**). Thus, these data demonstrate the immunosuppressive properties of the **IQ-1S**.

Molecular Pharmacology Fast Forward. Published on March 20, 2012 as DOI: 10.1124/mol.111.077446
This article has not been copyedited and formatted. The final version may differ from this version.

Discussion

The JNKs were isolated and characterized as stress-activated protein kinases on the basis of their activation in response to inhibition of protein synthesis (Johnson and Lapadat, 2002). Three distinct genes encoding JNK1, JNK2, and JNK3 have been identified, and at least 10 different splice variants exist in mammalian cells (Gupta et al., 2010). JNK1 and JNK2 are widely expressed in a variety of tissues, whereas JNK3 is selectively expressed in the brain and to a lesser extent in the heart and testis [reviewed in (Bogoyevitch et al., 2004)]. JNKs play a critical role in a wide range of diseases including apoptosis-related disorders (trauma, stroke, renal ischemia, neurodegenerative diseases) and inflammatory disorders (multiple sclerosis, rheumatoid arthritis, inflammatory bowel diseases) [reviewed in (Bogoyevitch et al., 2004;Zhang and Zhang, 2005)]. Studies of murine embryo fibroblasts demonstrate that loss of JNK causes major defects in cellular proliferation (Tournier et al., 2000). Moreover, dysregulated JNK may contribute to tumor development (Davis, 2000;Das et al., 2011). These observations, together with pharmacological studies using specific JNK inhibitors, indicate that JNKs are a key MAPK involved in the inflammatory response, neurodegenerative processes, and tumor growth. Thus, a large number of studies strongly support the notion that JNK inhibitors could serve as anti-inflammatory, anti-apoptotic drugs and might be developed as therapeutics [reviewed in (Bogoyevitch et al., 2004;Bogoyevitch et al., 2010)].

Because of the numerous potential clinical applications for JNK, many small molecule inhibitors have been described over the past three years, including piperazine amides (Shin et al., 2009), aminopyrazoles (Kamenecka et al., 2009), 1-aryl-3,4-dihydroisoquinolines (Christopher et al., 2009), quinazolines (He et al., 2011), and aminopurines (Plantevin Krenitsky et al., 2012). Here we report the identification of a novel series of oxime indenoquinoxalines that are relatively potent and highly specific JNK inhibitors. Cell-based assays, together with kinase profiling led

Molecular Pharmacology Fast Forward. Published on March 20, 2012 as DOI: 10.1124/mol.111.077446
This article has not been copyedited and formatted. The final version may differ from this version.

to the identification of five indenoquinoxalines (**IQ-1** through **IQ-4** and **IQ-1S**) with nanomolar JNK3 binding affinity and inhibitory activity for production of pro-inflammatory mediators in monocytes/macrophages and PBMCs. Indeed, binding experiments showed that these compounds had much higher affinity for JNK3 compared to JNK1/JNK2, CK1δ, PI3Kγ, and MKNK2. **IQ-1S** was also tested *in vivo* and was found to inhibit OVA-induced $CD4^+$ T-cell immune inflammation. Thus, these results suggest that the oxime indenoquinoxalines identified here exhibit the requirements of "lead-compounds", including the ability to cross biological membranes, lack of cytotoxicity, high degree of target specificity, and activity in *in vitro* cell-based systems and *in vivo*.

The indeno[1,2-b]quinoxaline nucleus has an extremely flat aromatic ring structure with a maximum deviation of 0.039 Å (Ghalib et al., 2010). Previously, the tri- and tetra-cyclic planar fragments have also been reported as kinase inhibitor scaffolds for Aurora A kinase (Warner et al., 2006) and JNK (Bennett et al., 2001). In general, flat ring structures have been identified as kinase-specific privileged structures, i.e., compounds containing these fragments are enriched for kinase targets, as compared to other target classes (Posy et al., 2011). In our additional screening, we found that compound **2** (2,3,8,9,10,11-hexahydro[1]benzothieno[2',3':4,5]pyrimido[1,2-a]azepine-4,13(1*H*,7*H*)-dione 4-(*O*-acetyloxime) had moderate binding activity for JNK1 and JNK3 and high binding activity for MKNK2. This compound has a planar nucleus, which is similar to tricyclic substructure of the 11*H*-indeno[1,2-b]quinoxaline tetracyclic moiety. Thus, other oximes with planar tri- or tetra-cyclic nuclei could be initial scaffolds for screening of additional kinase inhibitors.

Although the selected indenoquinoxalines exhibit similarity with JNK inhibitor SP600125 in the planarity of the core structure, they contain some unique features that can be exploited. From SAR analysis, we determined that the flexible side moiety R is critical for

Molecular Pharmacology Fast Forward. Published on March 20, 2012 as DOI: 10.1124/mol.111.077446
This article has not been copyedited and formatted. The final version may differ from this version.

biological activity and binding affinity of the indenoquinoxalines. Likewise, molecular docking results are in agreement with this observation and showed that polar atoms of the R substituent form H-bonds with JNK3 and that the indenoquinoxaline-derived JNK inhibitors were H-bonded mainly with Asn152, Gln155, or Met149 residues of JNK3.

From the kinase inhibition profile, we found that JNKs and CK1δ are the main kinase targets of **IQ-3**, although binding affinity for JNK3 was about 10-fold higher than for CK1δ. During recent years, several studies have highlighted the importance of JNK3 and CK1 isoforms in neurodegenerative diseases [reviewed in (Resnick and Fennell, 2004;Perez et al., 2011;Mehan et al., 2011)]. Thus, the dual JNK3/CK1δ inhibitory activity of indenoquinoxaline derivatives could be useful for application in treatment diseases such as Alzheimer's disease, where these kinases are implicated in different pathological pathways.

Several compounds with related indeno[1,2-b]quinoline and indolo[2,3-b]quinoxaline nuclei have been reported as inhibitors of topoisomerases I and II (Deady et al., 1997;Deady et al., 1999;Chen et al., 2000) and as cytotoxic compounds (Shibinskaya et al., 2010). However, the main effect of topoisomerase inhibitors is cytotoxicity, which was not found with our compounds and likely rules out topoisomerase inhibitory activity for these oxime quinoxalines. On the other hand, several related 11*H*-indeno[1,2-b]quinolin-11-one, 11*H*-indeno[1,2-b]quinoxaline, and 6*H*-indolo[2,3-b]quinoxaline derivatives have been reported to exhibit anti-inflammatory properties (Chojnacka-Wójcik and Naparzewska, 1983;Bala et al., 1986;Bala et al., 1983;Harbecke et al., 1999;Rajasekaran, 2007;Westman et al., 2008;Hultqvist et al., 2010), although the mechanism of the action was not determined. Our findings suggest the possibility that the anti-inflammatory effects reported for these derivatives may be due, in part, to inhibition of JNK activity. Clearly, further work is important to evaluate the JNK inhibitory activity of other analogs with anti-inflammatory properties, including Rabeximod and B-220.

In summary, we have identified a new class of kinase inhibitors, oxime derivatives of 11*H*-indeno[1,2-b]quinoxalines, that are potent and relatively specific JNK inhibitors. Indenoquinoxalines and other oxime derivatives represent new chemical tools that may be useful in further development of JNK inhibitors that could find application in disease models of inflammation and neurodegenerative diseases. Because of their potency and high specificity, these compounds represent important leads for the development of novel, potent and selective JNK inhibitors.

Molecular Pharmacology Fast Forward. Published on March 20, 2012 as DOI: 10.1124/mol.111.077446
This article has not been copyedited and formatted. The final version may differ from this version.

Acknowledgements

We thank KINOMEscan, Luceome Biotechnologies and Reaction Biology Corporation for kinase profiling, JNK3 enzyme kinetic assay, and consultation.

Authorship Contributions

Participated in research design: Schepetkin, Khlebnikov, Kochetkova, Pascual, Jutila, and Quinn.

Conducted experiments: Schepetkin, Kirpotina, Khlebnikov, Hanks, Kochetkova.

Contributed new reagents or analytic tools: Kochetkova and Pascual

Performed data analysis: Schepetkin, Khlebnikov, Kochetkova, Pascual, and Quinn.

Wrote or contributed to the writing of the manuscript: Schepetkin, Khlebnikov, Pascual, Jutila, and Quinn.

Molecular Pharmacology Fast Forward. Published on March 20, 2012 as DOI: 10.1124/mol.111.077446
This article has not been copyedited and formatted. The final version may differ from this version.

References

Albert DH, Tapang P, Magoc T J, Pease L J, Reuter D R, Wei R Q, Li J, Guo J, Bousquet P F, Ghoreishi-Haack N S, Wang B, Bukofzer G T, Wang Y C, Stavropoulos J A, Hartandi K, Niquette A L, Soni N, Johnson E F, McCall J O, Bouska J J, Luo Y, Donawho C K, Dai Y, Marcotte P A, Glaser K B, Michaelides M R and Davidsen S K (2006) Preclinical Activity of ABT-869, a Multitargeted Receptor Tyrosine Kinase Inhibitor. *Mol Cancer Ther* **5**:995-1006.

Atreya I, Atreya R and Neurath M F (2008) NF-κB in Inflammatory Bowel Disease. *J Intern Med* **263**:591-596.

Bain J, McLauchlan H, Elliott M and Cohen P (2003) The Specificities of Protein Kinase Inhibitors: an Update. *Biochem J* **371**:199-204.

Bala M, Michankow M, Chojnacka-Wójcik E, Wiczynska B and Tatarczynska E (1983) Chemistry and Anti-Inflammatory Activity of 10-Methylamino-11*H*-Indeno-[1,2-b]Quinolin-11-One (Mb 432) Derivatives. *Pol J Pharmacol Pharm* **35**:523-530.

Bala M, Naparzewska A and Chojnacka-Wójcik E (1986) Analgesic and Antiinflammatory Activity of 10-Amino-11*H*-Indeno-[1,2-b]Quinolin-11-One Derivatives. *Pol J Pharmacol Pharm* **38**:221-227.

Bennett BL, Sasaki D T, Murray B W, O'Leary E C, Sakata S T, Xu W, Leisten J C, Motiwala A, Pierce S, Satoh Y, Bhagwat S S, Manning A M and Anderson D W (2001) SP600125, an Anthrapyrazolone Inhibitor of Jun N-Terminal Kinase. *Proc Natl Acad Sci U S A* **98**:13681-13686.

Bennett BL, Satoh Y and Lewis A J (2003) JNK: a New Therapeutic Target for Diabetes. *Curr Opin Pharmacol* **3**:420-425.

Bhagwat SS (2007) MAP Kinase Inhibitors in Inflammation and Autoimmune Disorders. *Annu Rep Med Chem*265-278.

Bogoyevitch MA, Boehm I, Oakley A, Ketterman A J and Barr R K (2004) Targeting the JNK MAPK Cascade for Inhibition: Basic Science and Therapeutic Potential. *Biochim Biophys Acta* **1697**:89-101.

Bogoyevitch MA, Ngoei K R, Zhao T T, Yeap Y Y and Ng D C (2010) C-Jun N-Terminal Kinase (JNK) Signaling: Recent Advances and Challenges. *Biochim Biophys Acta* **1804**:463-475.

Carboni S, Hiver A, Szyndralewiez C, Gaillard P, Gotteland J P and Vitte P A (2004) AS601245 (1,3-Benzothiazol-2-Yl (2-[[2-(3-Pyridinyl) Ethyl] Amino]-4 Pyrimidinyl) Acetonitrile): a C-Jun NH_2-Terminal Protein Kinase Inhibitor With Neuroprotective Properties. *J Pharmacol Exp Ther* **310**:25-32.

Chambers JW, Pachori A, Howard S, Ganno M, Hansen D, Jr., Kamenecka T, Song X, Duckett D, Chen W, Ling Y Y, Cherry L, Cameron M D, Lin L, Ruiz C H and Lograsso P (2011) Small Molecule C-Jun-N-Terminal Kinase (JNK) Inhibitors Protect Dopaminergic Neurons in a Model of Parkinson's Disease. *ACS Chem Neurosci* **2**:198-206.

Chen CY, Gherzi R, Andersen J S, Gaietta G, Jurchott K, Royer H D, Mann M and Karin M (2000) Nucleolin and YB-1 Are Required for JNK-Mediated Interleukin-2 MRNA Stabilization During T-Cell Activation. *Genes Dev* **14**:1236-1248.

Chialda L, Zhang M, Brune K and Pahl A (2005) Inhibitors of Mitogen-Activated Protein Kinases Differentially Regulate Costimulated T Cell Cytokine Production and Mouse Airway Eosinophilia. *Respir Res* **6**:36.

Chojnacka-Wójcik E and Naparzewska A (1983) Pharmacological Properties of the Antiinflammatory Agent 10-Methylamine-11-H-Indeno-[1,2-b]Quinolin-11-One (Mb432). *Pol J Pharmacol Pharm* **35**:327-332.

Christopher JA, Atkinson F L, Bax B D, Brown M J, Champigny A C, Chuang T T, Jones E J, Mosley J E and Musgrave J R (2009) 1-Aryl-3,4-Dihydroisoquinoline Inhibitors of JNK3. *Bioorg Med Chem Lett* **19**:2230-2234.

Das M, Garlick D S, Greiner D L and Davis R J (2011) The Role of JNK in the Development of Hepatocellular Carcinoma. *Genes Dev* **25**:634-645.

Davis RJ (2000) Signal Transduction by the JNK Group of MAP Kinases. *Cell* **103**:239-252.

Deady LW, Desneves J, Kaye A J, Thompson M, Finlay G J, Baguley B C and Denny W A (1999) Ring-Substituted 11-Oxo-11*H*-Indeno[1,2-b]Quinoline-6-Carboxamides With Similar Patterns of Cytotoxicity to the Dual Topo I/II Inhibitor DACA. *Bioorg Med Chem* **7**:2801-2809.

Deady LW, Kaye A J, Finlay G J, Baguley B C and Denny W A (1997) Synthesis and Antitumor Properties of N-[2-(Dimethylamino)Ethyl]Carboxamide Derivatives of Fused Tetracyclic Quinolines and Quinoxalines: a New Class of Putative Topoisomerase Inhibitors. *J Med Chem* **40**:2040-2046.

Fabian MA, Biggs W H, III, Treiber D K, Atteridge C E, Azimioara M D, Benedetti M G, Carter T A, Ciceri P, Edeen P T, Floyd M, Ford J M, Galvin M, Gerlach J L, Grotzfeld R M, Herrgard S, Insko D E, Insko M A, Lai A G, Lelias J M, Mehta S A, Milanov Z V, Velasco A M, Wodicka L M, Patel H K, Zarrinkar P P and Lockhart D J (2005) A Small Molecule-Kinase Interaction Map for Clinical Kinase Inhibitors. *Nat Biotechnol* **23**:329-336.

Fujioka S, Niu J, Schmidt C, Sclabas G M, Peng B, Uwagawa T, Li Z, Evans D B, Abbruzzese J L and Chiao P J (2004) NF-κB and AP-1 Connection: Mechanism of NF-κB-Dependent Regulation of AP-1 Activity. *Mol Cell Biol* **24**:7806-7819.

Gaillard P, Jeanclaude-Etter I, Ardissone V, Arkinstall S, Cambet Y, Camps M, Chabert C, Church D, Cirillo R, Gretener D, Halazy S, Nichols A, Szyndralewiez C, Vitte P A and Gotteland J P (2005) Design and Synthesis of the First Generation of Novel Potent, Selective, and in Vivo Active (Benzothiazol-2-Yl)Acetonitrile Inhibitors of the C-Jun N-Terminal Kinase. *J Med Chem* **48**:4596-4607.

Ghalib RM, Hashim R, Sulaiman O, Hemamalini M and Fun H K (2010) 11*H*-Indeno-[1,2-b]Quinoxalin-11-One. *Acta Crystallogr Sect E Struct Rep Online* **66**:o1494.

Ghosh S and Hayden M S (2008) New Regulators of NF-κB in Inflammation. *Nat Rev Immunol* **8**:837-848.

Gupta SC, Sundaram C, Reuter S and Aggarwal B B (2010) Inhibiting NF-κB Activation by Small Molecules As a Therapeutic Strategy. *Biochim Biophys Acta* **1799**:775-787.

Han Z, Boyle D L, Chang L, Bennett B, Karin M, Yang L, Manning A M and Firestein G S (2001) C-Jun N-Terminal Kinase Is Required for Metalloproteinase Expression and Joint Destruction in Inflammatory Arthritis. *J Clin Invest* **108**:73-81.

Harbecke O, Dahlgren C, Bergman J and Moller L (1999) The Synthetic Non-Toxic Drug 2,3-Dimethyl-6(2-Dimethylaminoethyl)-6H-Indolo-(2,3-b)Quinoxaline Inhibits Neutrophil Production of Reactive Oxygen Species. *J Leukoc Biol* **65**:771-777.

He Y, Kamenecka T M, Shin Y, Song X, Jiang R, Noel R, Duckett D, Chen W, Ling Y Y, Cameron M D, Lin L, Khan S, Koenig M and LoGrasso P V (2011) Synthesis and SAR of Novel Quinazolines As Potent and Brain-Penetrant C-Jun N-Terminal Kinase (JNK) Inhibitors. *Bioorg Med Chem Lett* **21**:1719-1723.

Hibi M, Lin A, Smeal T, Minden A and Karin M (1993) Identification of an Oncoprotein- and UV-Responsive Protein Kinase That Binds and Potentiates the C-Jun Activation Domain. *Genes Dev* **7**:2135-2148.

Hultqvist M, Nandakumar K S, Bjorklund U and Holmdahl R (2010) Rabeximod Reduces Arthritis Severity in Mice by Decreasing Activation of Inflammatory Cells. *Ann Rheum Dis* **69**:1527-1532.

Jester BW, Cox K J, Gaj A, Shomin C D, Porter J R and Ghosh I (2010) A Coiled-Coil Enabled Split-Luciferase Three-Hybrid System: Applied Toward Profiling Inhibitors of Protein Kinases. *J Am Chem Soc* **132**:11727-11735.

Johnson GL and Lapadat R (2002) Mitogen-Activated Protein Kinase Pathways Mediated by ERK, JNK, and P38 Protein Kinases. *Science* **298**:1911-1912.

Jung DH, Park H J, Byun H E, Park Y M, Kim T W, Kim B O, Um S H and Pyo S (2010) Diosgenin Inhibits Macrophage-Derived Inflammatory Mediators Through Downregulation of CK2, JNK, NF-κB and AP-1 Activation. *Int Immunopharmacol* **10**:1047-1054.

Kalia J and Raines R T (2008) Hydrolytic Stability of Hydrazones and Oximes. *Angew Chem Int Ed Engl* **47**:7523-7526.

Kamenecka T, Habel J, Duckett D, Chen W, Ling Y Y, Frackowiak B, Jiang R, Shin Y, Song X and Lograsso P (2009) Structure-Activity Relationships and X-Ray Structures Describing the Selectivity of Aminopyrazole Inhibitors for C-Jun N-Terminal Kinase 3 (JNK3) Over P38. *J Biol Chem* **284**:12853-12861.

Kang MI, Henrich C J, Bokesch H R, Gustafson K R, McMahon J B, Baker A R, Young M R and Colburn N H (2009) A Selective Small-Molecule Nuclear Factor-κB Inhibitor From a High-Throughput Cell-Based Assay for "Activator Protein-1 Hits". *Mol Cancer Ther* **8**:571-581.

Karaman MW, Herrgard S, Treiber D K, Gallant P, Atteridge C E, Campbell B T, Chan K W, Ciceri P, Davis M I, Edeen P T, Faraoni R, Floyd M, Hunt J P, Lockhart D J, Milanov Z V, Morrison M J, Pallares G, Patel H K, Pritchard S, Wodicka L M and Zarrinkar P P (2008) A Quantitative Analysis of Kinase Inhibitor Selectivity. *Nat Biotechnol* **26**:127-132.

Kikkert R, de Groot E R and Aarden L A (2008) Cytokine Induction by Pyrogens: Comparison of Whole Blood, Mononuclear Cells, and TLR-Transfectants. *J Immunol Methods* **336**:45-55.

Kirpotina LN, Khlebnikov A I, Schepetkin I A, Ye R D, Rabiet M J, Jutila M A and Quinn M T (2010) Identification of Novel Small-Molecule Agonists for Human Formyl Peptide Receptors and Pharmacophore Models of Their Recognition. *Mol Pharmacol* **77**:159-170.

Kochetkova I, Golden S, Holderness K, Callis G and Pascual D W (2010) IL-35 Stimulation of $CD39^+$ Regulatory T Cells Confers Protection Against Collagen II-Induced Arthritis Via the Production of IL-10. *J Immunol* **184**:7144-7153.

Kornhuber J, Muehlbacher M, Trapp S, Pechmann S, Friedl A, Reichel M, Muhle C, Terfloth L, Groemer T W, Spitzer G M, Liedl K R, Gulbins E and Tripal P (2011) Identification of Novel Functional Inhibitors of Acid Sphingomyelinase. *PLoS One* **6**:e23852.

Law M, Corsino P, Parker N T and Law B K (2010) Identification of a Small Molecule Inhibitor of Serine 276 Phosphorylation of the P65 Subunit of NF-κB Using in Silico Molecular Docking. *Cancer Lett* **291**:217-224.

Mehan S, Meena H, Sharma D and Sankhla R (2011) JNK: a Stress-Activated Protein Kinase Therapeutic Strategies and Involvement in Alzheimer's and Various Neurodegenerative Abnormalities. *J Mol Neurosci* **43**:376-390.

Melino M, Hii C S, McColl S R and Ferrante A (2008) The Effect of the JNK Inhibitor, JIP Peptide, on Human T Lymphocyte Proliferation and Cytokine Production. *J Immunol* **181**:7300-7306.

Moreau A, Le V M, Jouan E, Parmentier Y and Fardel O (2011) Drug Transporter Expression in Human Macrophages. *Fundam Clin Pharmacol* **25**:743-752.

Nijboer CH, van der Kooij M A, van B F, Ohl F, Heijnen C J and Kavelaars A (2010) Inhibition of the JNK/AP-1 Pathway Reduces Neuronal Death and Improves Behavioral Outcome After Neonatal Hypoxic-Ischemic Brain Injury. *Brain Behav Immun* **24**:812-821.

Obot IB and Obi-Egbedi N O (2010) Indeno-1-One [2,3-b]Quinoxaline As an Effective Inhibitor for the Corrosion of Mild Steel in 0.5 M H_2SO_4 Solution. *Mater Chem Phys* **122**:325-328.

Oh KS, Lee S, Choi J K and Lee B H (2010) Identification of Novel Scaffolds for IκB Kinase Beta Inhibitor Via a High-Throughput Screening TR-FRET Assay. *Comb Chem High Throughput Screen* **13**:790-797.

Pearson BD (1962) Indenoquinolines. III. Derivatives of 11*H*-Indeno-[1,2-b]Quinoxaline and Related Indenoquinolines. *J Org Chem* **27**:1674-&.

Peddibhotla S, Shi R, Khan P, Smith L H, Mangravita-Novo A, Vicchiarelli M, Su Y, Okolotowicz K J, Cashman J R, Reed J C and Roth G P (2010) Inhibition of Protein Kinase C-Driven Nuclear Factor-κB Activation: Synthesis, Structure-Activity Relationship, and Pharmacological Profiling of Pathway Specific Benzimidazole Probe Molecules. *J Med Chem* **53**:4793-4797.

Peng SL (2008) Transcription Factors in Autoimmune Diseases. *Front Biosci* **13**:4218-4240.

Perez DI, Gil C and Martinez A (2011) Protein Kinases CK1 and CK2 As New Targets for Neurodegenerative Diseases. *Med Res Rev* **31**:924-954.

Plantevin Krenitsky V, Nadolny L, Delgado M, Ayala L, Clareen S S, Hilgraf R, Albers R, Hegde S, D'Sidocky N, Sapienza J, Wright J, McCarrick M, Bahmanyar S, Chamberlain P, Delker S L, Muir J, Giegel D, Xu L, Celeridad M, Lachowitzer J, Bennett B, Moghaddam M, Khatsenko O, Katz J, Fan R, Bai A, Tang Y, Shirley M A, Benish B, Bodine T, Blease K, Raymon H, Cathers B E and Satoh Y (2012) Discovery of CC-930, an Orally Active Anti-Fibrotic JNK Inhibitor. *Bioorg Med Chem Lett* **22**:1433-1438.

Posy SL, Hermsmeier M A, Vaccaro W, Ott K H, Todderud G, Lippy J S, Trainor G L, Loughney D A and Johnson S R (2011) Trends in Kinase Selectivity: Insights for Target Class-Focused Library Screening. *J Med Chem* **54**:54-66.

Rajasekaran A (2007) Synthesis, Antinociceptive, Antiinflammatory and Antiepileptic Evaluation of Some Novel Indeno[1,2-b]Quinoxalin-11-Ylidenamines. *Iran J Pharm Sci* **3**:251-262.

Resnick L and Fennell M (2004) Targeting JNK3 for the Treatment of Neurodegenerative Disorders. *Drug Discov Today* **9**:932-939.

Sabapathy K, Hu Y, Kallunki T, Schreiber M, David J P, Jochum W, Wagner E F and Karin M (1999) JNK2 Is Required for Efficient T-Cell Activation and Apoptosis but Not for Normal Lymphocyte Development. *Curr Biol* **9**:116-125.

Schepetkin IA, Khlebnikov A I, Kirpotina L N and Quinn M T (2006) Novel Small-Molecule Inhibitors of Anthrax Lethal Factor Identified by High-Throughput Screening. *J Med Chem* **49**:5232-5244.

Schepetkin IA, Khlebnikov A I and Quinn M T (2007a) *N*-Benzoylpyrazoles Are Novel Small-Molecule Inhibitors of Human Neutrophil Elastase. *J Med Chem* **50**:4928-4938.

Schepetkin IA, Kirpotina L N, Jakiw L, Khlebnikov A I, Blaskovich C L, Jutila M A and Quinn M T (2009) Immunomodulatory Activity of Oenothein B Isolated From *Epilobium Angustifolium*. *J Immunol* **183**:6754-6766.

Schepetkin IA, Kirpotina L N, Khlebnikov A I and Quinn M T (2007b) High-Throughput Screening for Small-Molecule Activators of Neutrophils: Identification of Novel N-Formyl Peptide Receptor Agonists. *Mol Pharmacol* **71**:1061-1074.

Shibinskaya MO, Lyakhov S A, Mazepa A V, Andronati S A, Turov A V, Zholobak N M and Spivak N Y (2010) Synthesis, Cytotoxicity, Antiviral Activity and Interferon Inducing Ability of 6-(2-Aminoethyl)-6H-Indolo[2,3-b]Quinoxalines. *Eur J Med Chem* **45**:1237-1243.

Shin Y, Chen W, Habel J, Duckett D, Ling Y Y, Koenig M, He Y, Vojkovsky T, Lograsso P and Kamenecka T M (2009) Synthesis and SAR of Piperazine Amides As Novel C-Jun N-Terminal Kinase (JNK) Inhibitors. *Bioorg Med Chem Lett* **19**:3344-3347.

Skazik C, Heise R, Bostanci O, Paul N, Denecke B, Joussen S, Kiehl K, Merk H F, Zwadlo-Klarwasser G and Baron J M (2008) Differential Expression of Influx and Efflux Transport Proteins in Human Antigen Presenting Cells. *Exp Dermatol* **17**:739-747.

Szczepankiewicz BG, Kosogof C, Nelson L T, Liu G, Liu B, Zhao H, Serby M D, Xin Z, Liu M, Gum R J, Haasch D L, Wang S, Clampit J E, Johnson E F, Lubben T H, Stashko M A, Olejniczak E T, Sun C, Dorwin S A, Haskins K, Abad-Zapatero C, Fry E H, Hutchins C W, Sham H L, Rondinone C M and Trevillyan J M (2006) Aminopyridine-Based C-Jun N-Terminal Kinase Inhibitors With Cellular Activity and Minimal Cross-Kinase Activity. *J Med Chem* **49**:3563-3580.

Tournier C, Hess P, Yang D D, Xu J, Turner T K, Nimnual A, Bar-Sagi D, Jones S N, Flavell R A and Davis R J (2000) Requirement of JNK for Stress-Induced Activation of the Cytochrome C-Mediated Death Pathway. *Science* **288**:870-874.

Vaiopoulos AG, Papachroni K K and Papavassiliou A G (2010) Colon Carcinogenesis: Learning From NF-κB and AP-1. *Int J Biochem Cell Biol* **42**:1061-1065.

Vallières M and Du Souich P (2010) Modulation of Inflammation by Chondroitin Sulfate. *Osteoarthritis Cartilage* **18 Suppl 1**:S1-S6.

Wagner G and Laufer S (2006) Small Molecular Anti-Cytokine Agents. *Med Res Rev* **26**:1-62.

Warner SL, Bashyam S, Vankayalapati H, Bearss D J, Han H, Mahadevan D, Von Hoff D D and Hurley L H (2006) Identification of a Lead Small-Molecule Inhibitor of the Aurora Kinases Using a Structure-Assisted, Fragment-Based Approach. *Mol Cancer Ther* **5**:1764-1773.

Watanabe M, Nakashima M, Togano T, Higashihara M, Watanabe T, Umezawa K and Horie R (2008) Identification of the RelA Domain Responsible for Action of a New NF-κB Inhibitor DHMEQ. *Biochem Biophys Res Commun* **376**:310-314.

Westman E, Thi Ngoc D D, Klareskog L and Harris H E (2008) Suppressive Effects of a Quinoxaline-Analogue (Rob 803) on Pathogenic Immune Mechanisms in Collagen-Induced Arthritis. *Clin Exp Immunol* **152**:192-199.

Xie X, Gu Y, Fox T, Coll J T, Fleming M A, Markland W, Caron P R, Wilson K P and Su M S (1998) Crystal Structure of JNK3: a Kinase Implicated in Neuronal Apoptosis. *Structure* **6**:983-991.

Xie, X., Gu, Y., Markland, W., Su, M. S., Caron, P. R., Fox, E., and Wilson, K. P. Methods of designing inhibitors for JNK kinases. [Vertex Pharmaceuticals: US Patent 7383135]. 2008.
Ref Type: Patent

Yan C, Kaoud T, Lee S, Dalby K N and Ren P (2011) Understanding the Specificity of a Docking Interaction Between JNK1 and the Scaffolding Protein JIP1. *J Phys Chem B* **115**:1491-1502.

Yeste-Velasco M, Folch J, Casadesus G, Smith M A, Pallas M and Camins A (2009) Neuroprotection by C-Jun NH_2-Terminal Kinase Inhibitor SP600125 Against Potassium Deprivation-Induced Apoptosis Involves the Akt Pathway and Inhibition of Cell Cycle Reentry. *Neuroscience* **159**:1135-1147.

Zhang GY and Zhang Q G (2005) Agents Targeting C-Jun N-Terminal Kinase Pathway As Potential Neuroprotectants. *Expert Opin Investig Drugs* **14**:1373-1383.

Zoukhri D, Macari E, Choi S H and Kublin C L (2006) C-Jun NH_2-Terminal Kinase Mediates Interleukin-1β-Induced Inhibition of Lacrimal Gland Secretion. *J Neurochem* **96**:126-135.

Footnotes

This work was supported in part by grants from the National Institutes of Health [RR020185, GM103500, and AT004986], an equipment grant from the M.J. Murdock Charitable Trust, and the Montana State University Agricultural Experiment Station.

Molecular Pharmacology Fast Forward. Published on March 20, 2012 as DOI: 10.1124/mol.111.077446
This article has not been copyedited and formatted. The final version may differ from this version.

Figure Legends

Figure 1. Structure of and activity of **IQ-1** (11*H*-indeno[1,2-b]quinoxalin-11-one oxime). THP1-Blue monocytes (2 x 10^5 cells/well) were pretreated with the indicated concentrations of **IQ-1** or DMSO for 30 min, followed by addition of 200 ng/ml LPS or buffer for 24 h. Secreted alkaline phosphatase activity was analyzed spectrophotometrically in the cell supernatant (●, left axis). Cell viability was measured using the CellTiter-Glo Luminescent Cell Viability Assay Kit, and the results are expressed as % of DMSO control (○, right axis). The data are presented as the mean ±S.D. of triplicate samples from one experiment that is representative of three independent experiments.

Figure 2. Effect of the **IQ-1** on human PBMC cytokine production. PBMCs were pretreated with 20 μM of **IQ-1** or DMSO for 30 min, followed by addition of 200 ng/ml LPS or buffer for 24 h. Production of cytokines in the supernatants was evaluated using a semiquantity MultiAnalyte ELISArray kit. The relative level of cytokine production is shown as fold increase over background (DMSO control). The data are presented as the mean ±S.E.M. of duplicate samples from one experiment that is representative of two independent experiments.

Figure 3. Effect of the **IQ-1** and **IQ-3** on TNF-α production by human PBMCs. PBMCs were pretreated with the indicated compounds or DMSO for 30 min, followed by addition of 200 ng/ml LPS or buffer for 24 h. Production of TNF-α in the supernatants was evaluated by ELISA. The data are presented as the mean ±S.D. of triplicate samples from one experiment that is representative of three independent experiments.

Molecular Pharmacology Fast Forward. Published on March 20, 2012 as DOI: 10.1124/mol.111.077446
This article has not been copyedited and formatted. The final version may differ from this version.

Figure 4. Kinase profile of indenoquinoxaline **IQ-3**. Kinases marked with an asterisk (*****) were evaluated using Luceome Biotechnologies. The other kinases were evaluated using the KINOMEscan platform, as described under *Materials and Methods*. Shown is the % inhibition of binding to an active-site directed ligand for each of the indicated kinases after treatment with 10 μM **IQ-3**.

Figure 5. Pharmacological inhibition of c-Jun (S63) phosphorylation by selected indenoquinoxalines. Human MonoMac-6 monocytic cells were pretreated with 25 μM of **IQ-1** through **IQ-4**, **IQ-1S**, SP600125, **IQ-18** or DMSO vehicle (**Panel A**) or the indicated concentrations of **IQ-1** and **IQ-3** (**Panel B**) for 30 min, followed by treatment with LPS (200 ng/ml) or vehicle for another 30 min. The cells were lyses, and the lysates were analyzed by Western blotting as described (**Panel A**). GAPDH was used as the loading control for the lysates. The blots were analyzed by densitometry, and the ratio of phospho-c-Jun/total c-Jun is shown in (**Panel B**) for **IQ-1** and **IQ-3**. Representative blot and densitometric analysis from 3 independent experiments.

Figure 6. Molecular modeling of active inhibitors in the JNK3 binding site. **Panel A.** Binding poses for active inhibitors **IQ-1** (blue), **IQ-2** (white), **IQ-3** (magenta), and **IQ-4** (dark-brown) are shown. The binding site region is shown by surface color according to electrostatic properties (red or blue – positively or negatively charged areas, respectively). **Panel B** shows the same image viewed from the side with the left half of the binding cleft removed for ease of viewing the orientation of the compounds within the cleft.

Molecular Pharmacology Fast Forward. Published on March 20, 2012 as DOI: 10.1124/mol.111.077446
This article has not been copyedited and formatted. The final version may differ from this version.

Figure 7. Modeling H-bond interactions of active and non-active compounds in the JNK3 binding site. **Panel A**. Overlaid docking poses of **IQ-3** (magenta) and non-active compound **IQ-18** (red). **Panel B**. Overlaid docking poses of **IQ-3** (magenta) and known JNK inhibitor SP600125 (green). H-bonds are shown in green. Hydrogen atoms are removed for simplicity.

Figure 8. JNK inhibitors suppress OVA-specific DTH response. Sorted DO11.10 CD4+ T-cells were adoptively transferred into BALB/c mice (10-13 mice per group). One day later, the recipients were challenged with 100 μg OVA, and the mice were treated (i.p.) every 12 hr with 12.5 mg/kg inhibitor or vehicle control for a total of 5 injections. On day 5, the DTH test was performed as described under *Material and Methods,* and 24 hrs later ear thickness was measured (mean change in ear thickness for each animal is shown). Mann-Whitney *U* test was used for statistical analysis of DTH response. *$p<0.05$ indicates statistically significant difference in ear thickness between treatment groups.

Molecular Pharmacology Fast Forward. Published on March 20, 2012 as DOI: 10.1124/mol.111.077446
This article has not been copyedited and formatted. The final version may differ from this version.

Table 1. Effect of indenoquinoxaline derivatives on LPS-induced NF-κB/AP-1 transcriptional activity and cytotoxicity in human THP-1Blue monocytic cells[a]

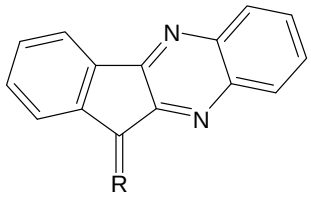

IQ#	R	NF-κB/ AP-1 IC_{50} (μM)	Toxicity IC_{50} (μM)	IQ#	R	NF-κB/ AP-1 IC_{50} (μM)	Toxicity IC_{50} (μM)
1S	=N-ONa	1.8 ± 0.3	N.T.	**10**	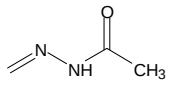	3.6 ± 0.72	N.T.
2	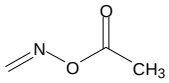	0.90 ± 0.21	N.T.	**11**	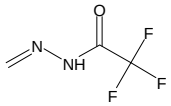	N.A.	N.T.
3	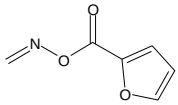	1.4 ± 0.42	N.T.	**12**	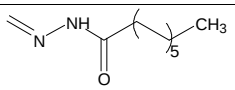	N.A.	N.T.
4	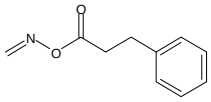	0.92 ± 0.33	N.T.	**13**	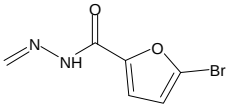	N.A.	N.T.
5	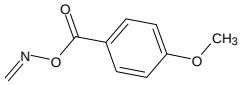	6.7 ± 1.4	N.T.	**14**	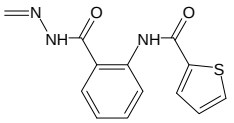	N.A.	N.T.
6	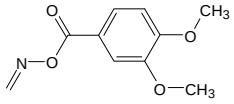	4.9 ± 1.1	N.T.	**15**	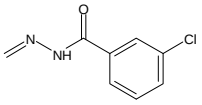	N.A.	N.T.
7		3.7 ± 0.72	N.T.	**16**	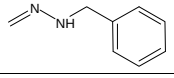	N.A.	N.T.
8	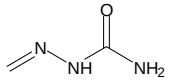	2.3 ± 0.54	N.T.	**17**	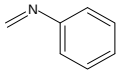	N.A.	N.T.
9	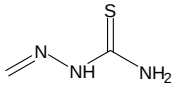	3.1 ± 0.60	N.T.	**18**		N.A.	N.T.

[a]THP-1Blue monocytic cells were treated with the indicated compounds, activated with 200 ng/ml LPS, and secreted alkaline phosphatase reporter activity was monitored. N.A., no inhibition of reporter activity at concentrations <40 μM. N.T., non-toxic at concentrations <40 μM.

Molecular Pharmacology Fast Forward. Published on March 20, 2012 as DOI: 10.1124/mol.111.077446
This article has not been copyedited and formatted. The final version may differ from this version.

Table 2. Effect of selected indenoquinoxalines on LPS-induced production of TNF-α, IL-6, and NO by PBMCs, MonoMac-6 cells, and J774.A1 cells and evaluation of cytotoxicity[a]

IQ#	Human MonoMac-6 cells			Human PBMCs			Murine J774.A1	
	TNF-α	IL-6	Toxicity	TNF-α	IL-6	Toxicity	NO	Toxicity
	IC_{50} (μM)							
1	1.3 ± 0.31	3.8 ± 0.78	N.T.	2.6 ± 0.63	5.6 ± 1.1	N.T.	3.1± 0.87	N.T.
1S	0.25 ± 0.11	0.61 ± 0.15	N.T.	2.0 ± 0.27	7.1 ± 2.6	N.T.	12.5 ± 4.4	N.T.
2	1.2 ± 0.19	1.6 ± 0.33	N.T.	3.7 ± 0.78	5.1 ± 1.2	N.T.	4.7 ± 1.2	N.T.
3	2.2 ± 0.36	1.5 ± 0.41	N.T.	4.7 ± 1.2	9.1 ± 1.9	N.T.	6.4 ± 2.1	N.T.
4	2.0 ± 0.32	3.1 ± 0.47	N.T.	4.9 ± 1.1	10.3± 2.1	N.T.	9.4 ± 2.6	N.T.
5	1.2 ± 0.21	2.4 ± 0.42	N.T.	10.2 ± 2.4	N.A.	N.T.	N.A.	N.T.
6	0.32 ± 0.12	1.7 ± 0.37	N.T.	N.A.	N.A.	N.T.	N.A.	N.T.
7	5.6 ± 1.1	8.5 ± 0.93	N.T.	8.5 ± 1.7	19.7± 4.2	N.T.	N.A.	N.T.
8	4.2 ± 0.88	3.5 ± 0.80	N.T.	3.4 ± 0.72	5.1 ± 1.2	N.T.	N.A.	26.2± 4.3
9	6.2 ± 1.4	7.9 ± 1.66	N.T.	2.8 ± 0.55	N.A.	16.1 ± 3.1	N.A.	N.T.
10	12.6 ± 2.6	N.A.	N.T.	6.2 ± 1.3	N.A.	N.T.	N.A.	N.T.
13	N.A.	N.A.	N.T.	N.A.	N.A.	N.T.	N.A.	N.T.
15	N.A.	N.A.	N.T.	N.A.	N.A.	N.T.	N.A.	N.T.
18	N.A.	N.A.	N.T.	N.A.	N.A.	N.T.	N.A.	N.T.

[a]Cells were treated with test compounds and activated with 200 ng/ml of LPS. N.A., no inhibition at concentrations <40 μM. N.T., non-toxic at concentrations <40 μM; the indicated values for cell toxicity are expressed as IC_{50} for reduction in cell viability.

Molecular Pharmacology Fast Forward. Published on March 20, 2012 as DOI: 10.1124/mol.111.077446
This article has not been copyedited and formatted. The final version may differ from this version.

Table 3. Effect of selected kinase inhibitors on LPS-induced TNF-α production in MonoMac-6 cells and human PBMCs[a]

Inhibitor	Target Kinase	MonoMac-6	PBMCs
		IC_{50} (μM)	
PF670462	CK1ε/CK1δ	2.8 ± 0.89	2.4 ± 0.78
AS252424	PI3Kγ	No effect	No effect
AS605240	PI3Kγ	No effect	No effect
TCSPIM-1 1	PIM-1	No effect	No effect
SP600125	JNKs	6.3 ± 2.6	5.7 ± 2.1

[a]Cells were treated with indicated inhibitors, activated with 200 ng/ml LPS, and TNF-α production was monitored.

Molecular Pharmacology Fast Forward. Published on March 20, 2012 as DOI: 10.1124/mol.111.077446
This article has not been copyedited and formatted. The final version may differ from this version.

Table 4. Binding affinity of the most active indenoquinoxaline derivatives and JNK inhibitor SP600125 toward selected kinases

Compound	JNK1	JNK2	JNK3	CK1δ	PI3Kγ	MKNK2
	K_d (μM)[a]					
IQ-1	0.24	0.36	0.10	0.38	0.47	0.92
IQ-1S	0.39	0.36	0.087	1.4	1.2	1.8
IQ-2	0.33	0.48	0.09	0.66	0.58	1.2
IQ-3	0.24	0.29	0.066	0.56	0.43	1.2
IQ-4	0.44	0.58	0.12	0.66	0.76	1.8
IQ-6	0.27	0.28	0.064	5.7	12.0	40.0
SP600125[b]	0.10	0.084	0.022	-	-	1.0

[a] K_d values were determined by KINOMEscan. [b] K_d for SP600125, determined on same platform, was previously published (Fabian et al., 2005).

Molecular Pharmacology Fast Forward. Published on March 20, 2012 as DOI: 10.1124/mol.111.077446
This article has not been copyedited and formatted. The final version may differ from this version.

Table 5. H-bonding centers in JNK3 and docked molecules and energies of H-bonds between the indicated centers for the best predicted docking poses.

	IQ#	Number of H-bonds	Ligand (type of H-bonding center)	JNK3 Residues (type of H-bonding center)	Energy (kcal/mo
Active Compounds	**1**	2	Oxime nitrogen (A[a])	NH_2 group of **Asn152** side chain (D)	1.11
			Oxime OH (D)	Backbone C=O of **Ile70** (A)	3.52
	2	1	Protonated C=O in acetyl (D)	C=O of **Asn194** side chain (A)	3.88
	3	2	NH in protonated heterocycle (D)	C=O of **Gln155** side chain (A)	1.39
			Oxime nitrogen and oxygen (A)	NH_2 group of **Asn152** side chain (D)	3.08
	4	1	Oxime oxygen (A)	NH_2 group of **Asn152** side chain (D)	1.13
	5	3	Oxime nitrogen and oxygen (A)	Protonated amino group of **Lys93** side chain (D)	4.70
			NH in protonated heterocycle (D)	OH of **Ser193** (A)	1.82
			Methoxy oxygen (A)	Amino group of **Asn152** side chain (D)	0.49
	6	2	Protonated C=O of acyloxime (D)	C=O of **Gln155**side chain (A)	5.87
			NH in protonated heterocycle (D)	Backbone C=O of **Ile70** (A)	0.69
	7	2	Terminal NH_2 group (D)	C=O of **Gln155** side chain (A)	5.68
			NH in protonated heterocycle (D)	Backbone C=O of **Ile70** (A)	0.25
Inactive Compounds	**8**	2	Protonated C=O group (D)	C=O of **Asn194** side chain (A)	0.26
			Two nitrogen atoms of hydrazone moiety (A)	Protonated amino group of **Lys93** side chain (D)	0.74
	9	2	Terminal NH_2 group (D)	Backbone C=O of **Gly76** (A)	1.10
			NH in protonated heterocycle (D)	C=O of **Gln155** side chain (A)	1.53
	10	2	C=O group and imine nitrogen of hydrazone moiety (A)	NH_2 group of **Asn152** side chain (D)	0.37
			NH in hydrazone moiety (D)	Backbone C=O of **Ser72** (A)	0.50
	11	2	C=O group and NH in hydrazone moiety (A)	Protonated amino group of **Lys93** side chain (D)	2.55
			NH in protonated heterocycle (D)	Backbone C=O of **Ser72** (acceptor)	0.21
	13	1	Furan oxygen (A)	Protonated NH_2 group of **Lys93** side chain (D	2.49
	15	2	C=O group (A)	Protonated NH_2 group of **Lys93** side chain (D)	2.33
			NH in protonated heterocycle (D)	Backbone C=O of **Ile70** (A)	0.70
	16	0	-	-	-
	17	0	-	-	-
	18	1	Protonated C=O (D)	Backbone C=O of **Met149** (A)	1.56

[a]Donor and acceptor types of H-bonding centers are abbreviated as D and A, respectively.

Figure 1

A

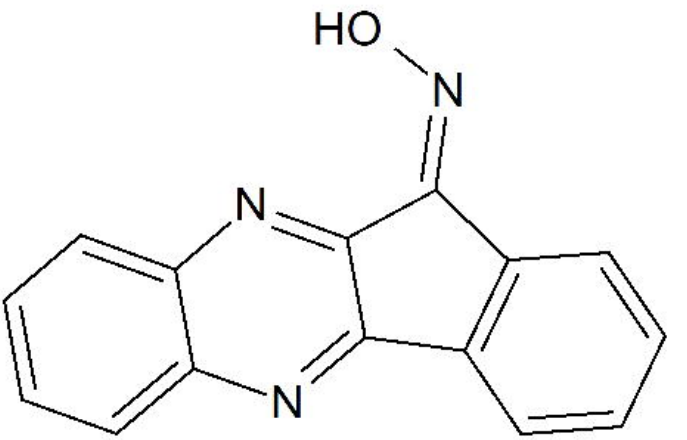

Compound **IQ-1**

B

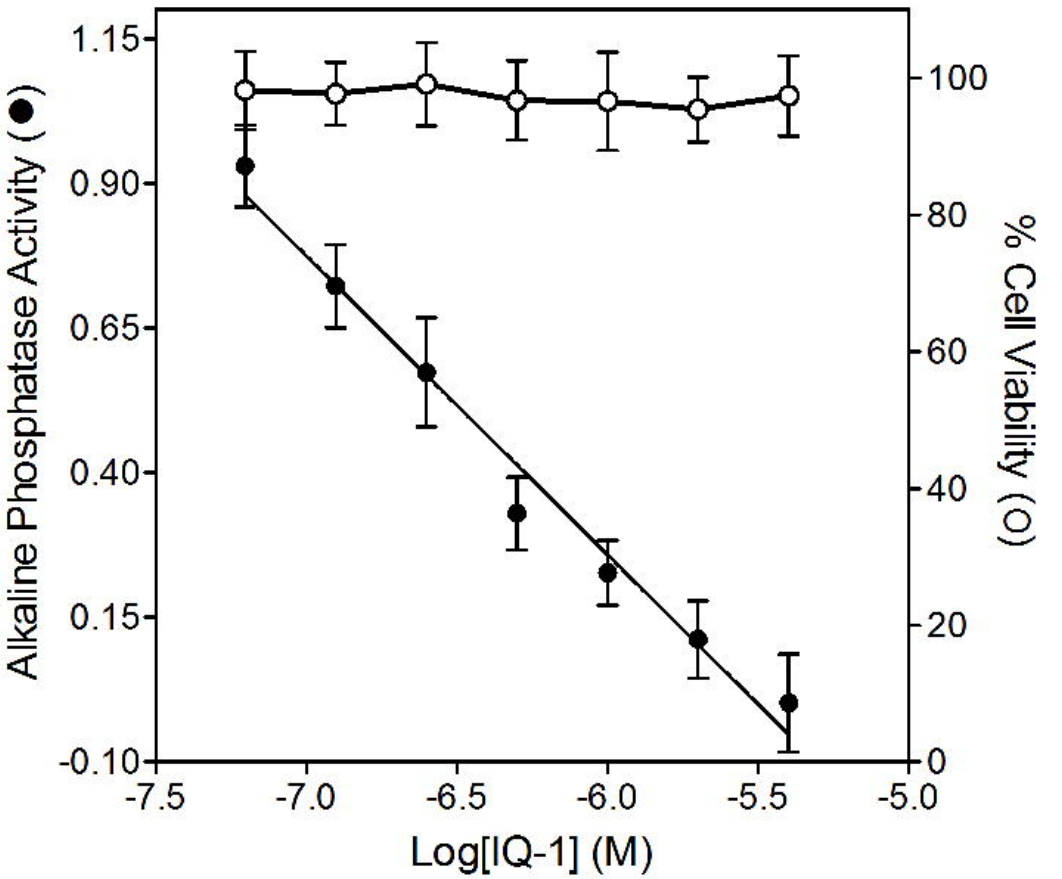

Figure 2

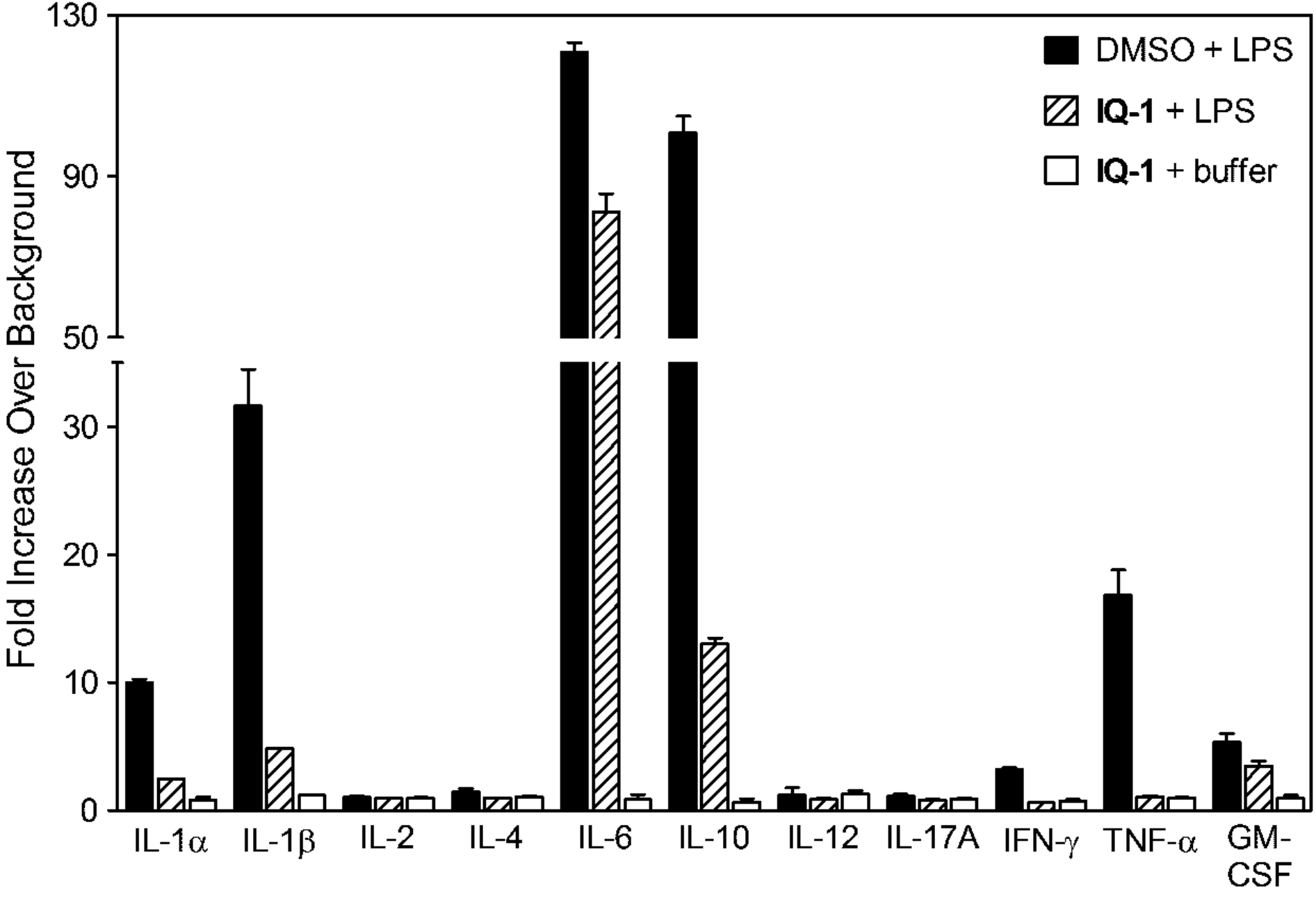
130
90
50
30
20
10
0
Fold Increase Over Background
DMSO + LPS
IQ-1 + LPS
IQ-1 + buffer
IL-1α
IL-1β
IL-2
IL-4
IL-6
IL-10
IL-12
IL-17A
IFN-γ
TNF-α
GM-CSF

Figure 3

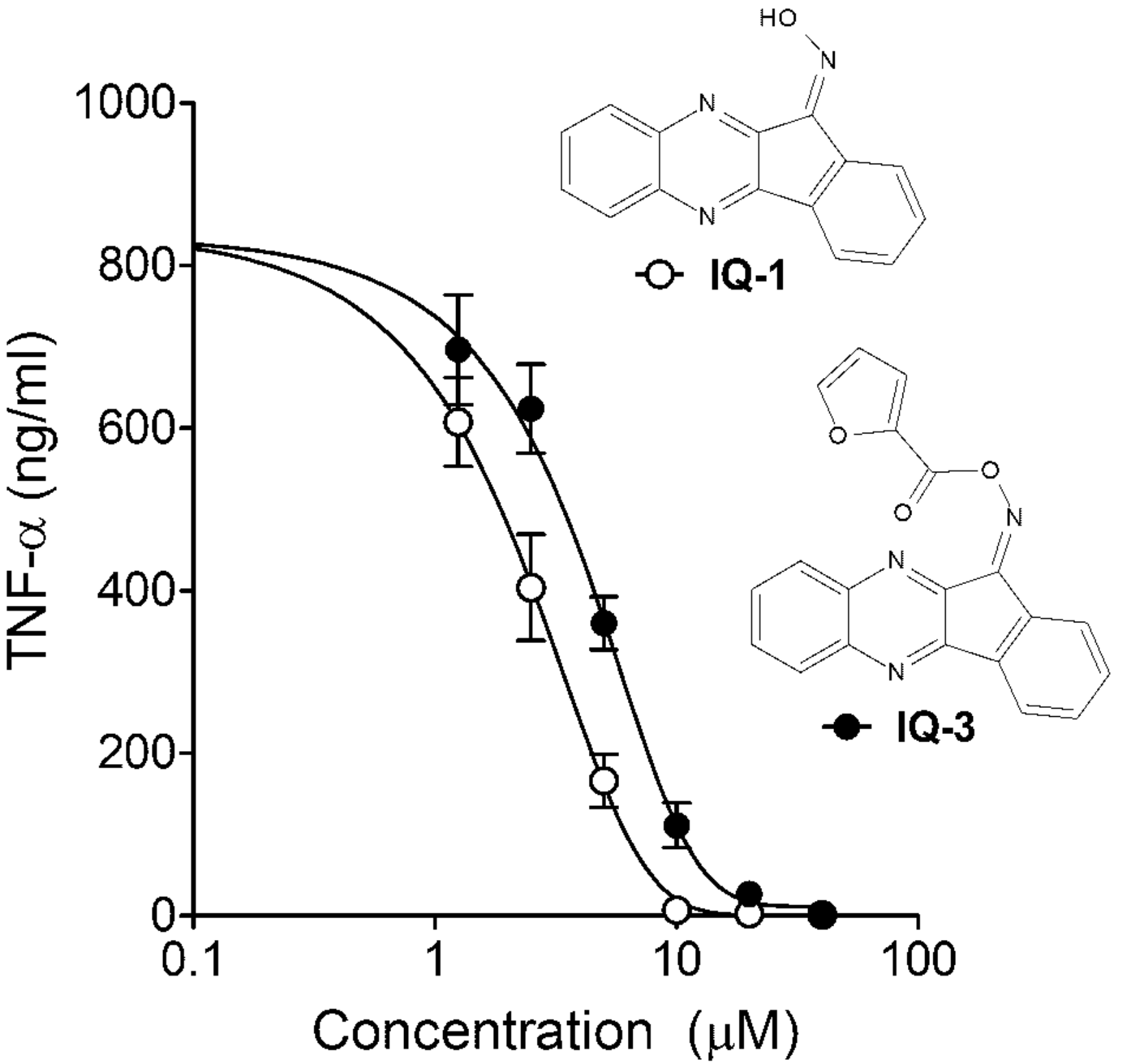
HO
N
N
N
IQ-1
O
O
O
N
N
N
IQ-3
1000
800
600
400
200
0
TNF-α (ng/ml)
0.1
1
10
100
Concentration (μM)

Molecular Pharmacology Fast Forward. Published on March 20, 2012 as DOI: 10.1124/mol.111.077446
This article has not been copyedited and formatted. The final version may differ from this version.

Figure 4

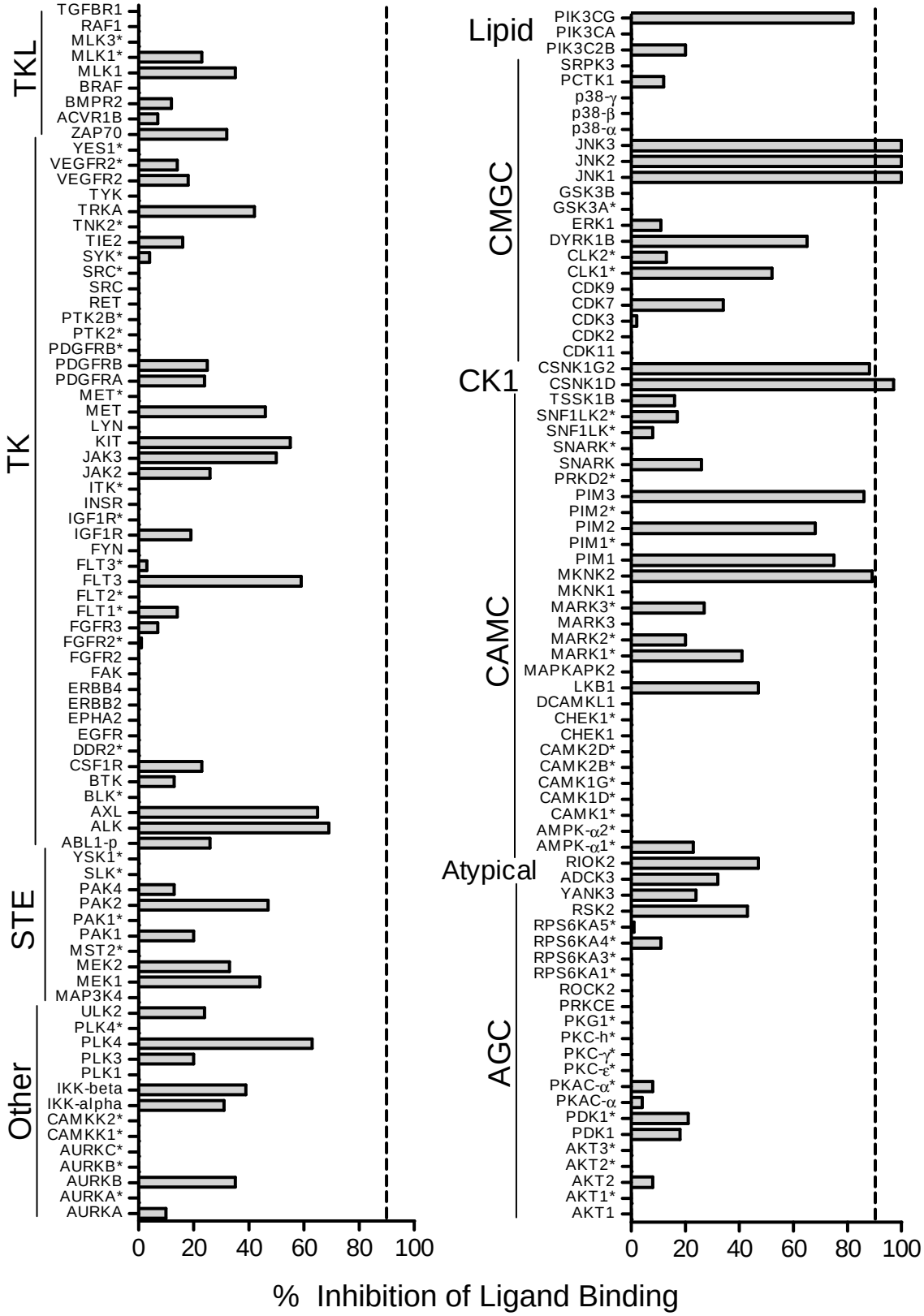

Molecular Pharmacology Fast Forward. Published on March 20, 2012 as DOI: 10.1124/mol.111.077446
This article has not been copyedited and formatted. The final version may differ from this version.

Figure 5

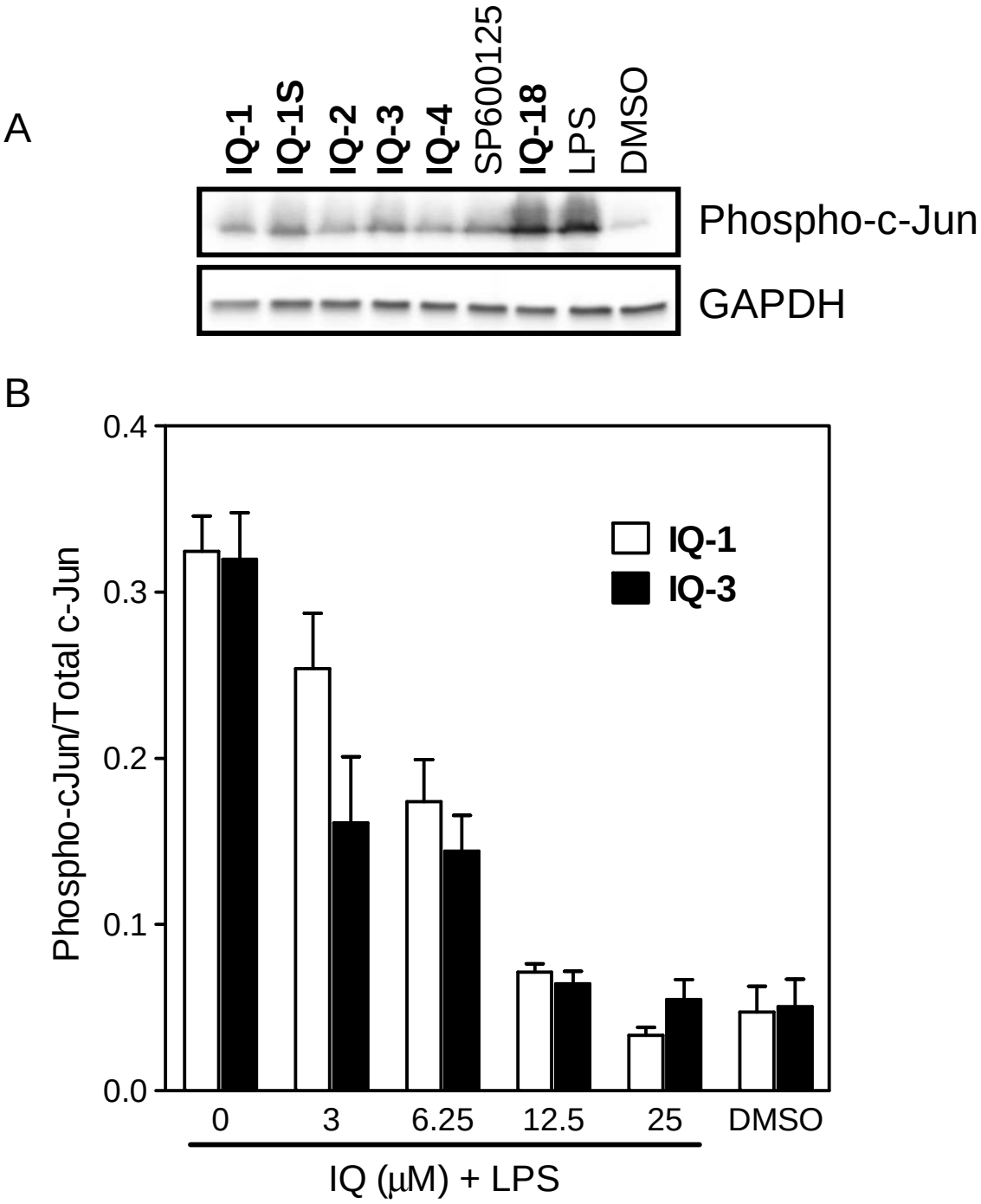

Molecular Pharmacology Fast Forward. Published on March 20, 2012 as DOI: 10.1124/mol.111.077446
This article has not been copyedited and formatted. The final version may differ from this version.

Figure 6

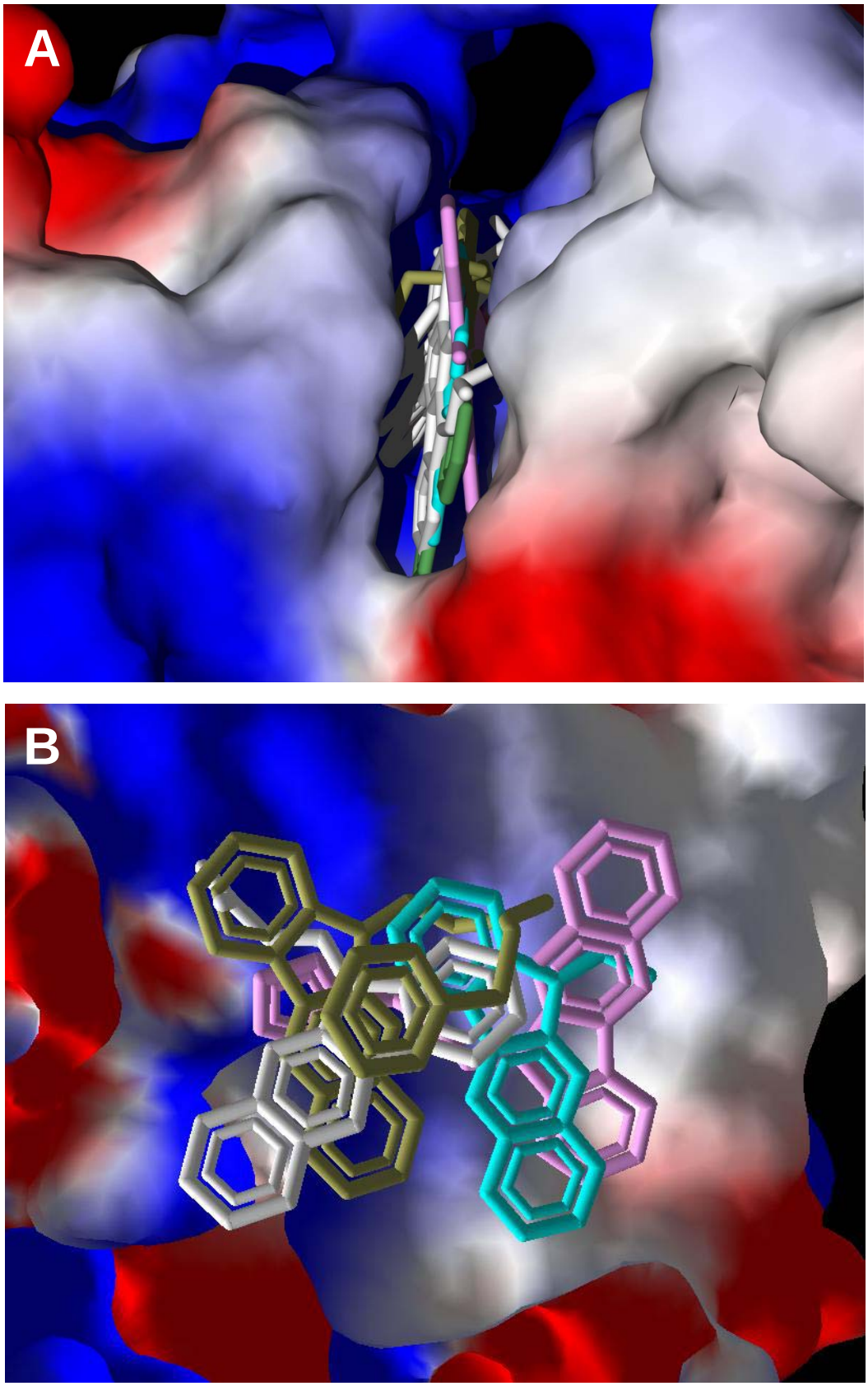

Molecular Pharmacology Fast Forward. Published on March 20, 2012 as DOI: 10.1124/mol.111.077446
This article has not been copyedited and formatted. The final version may differ from this version.

Figure 7

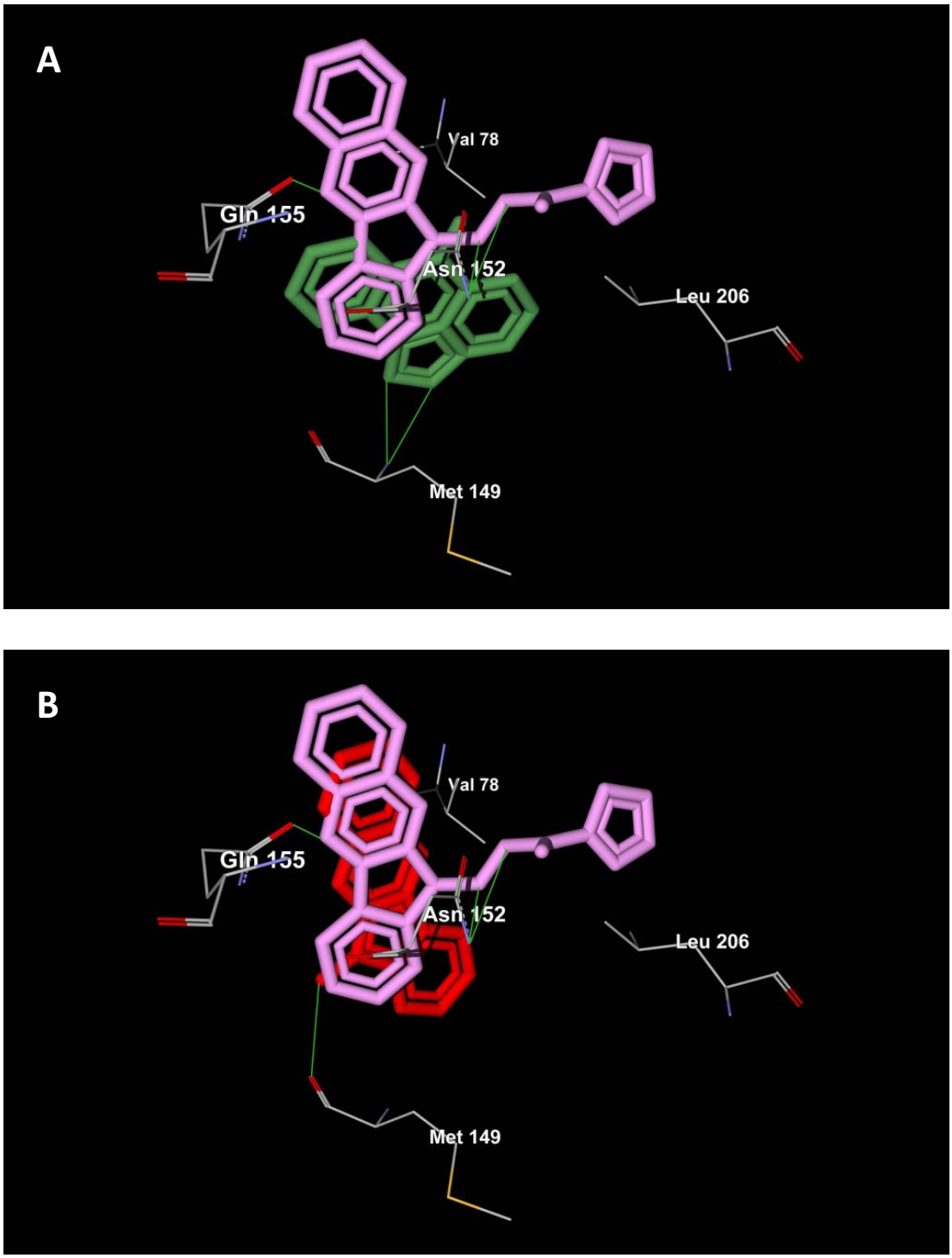

Figure 8

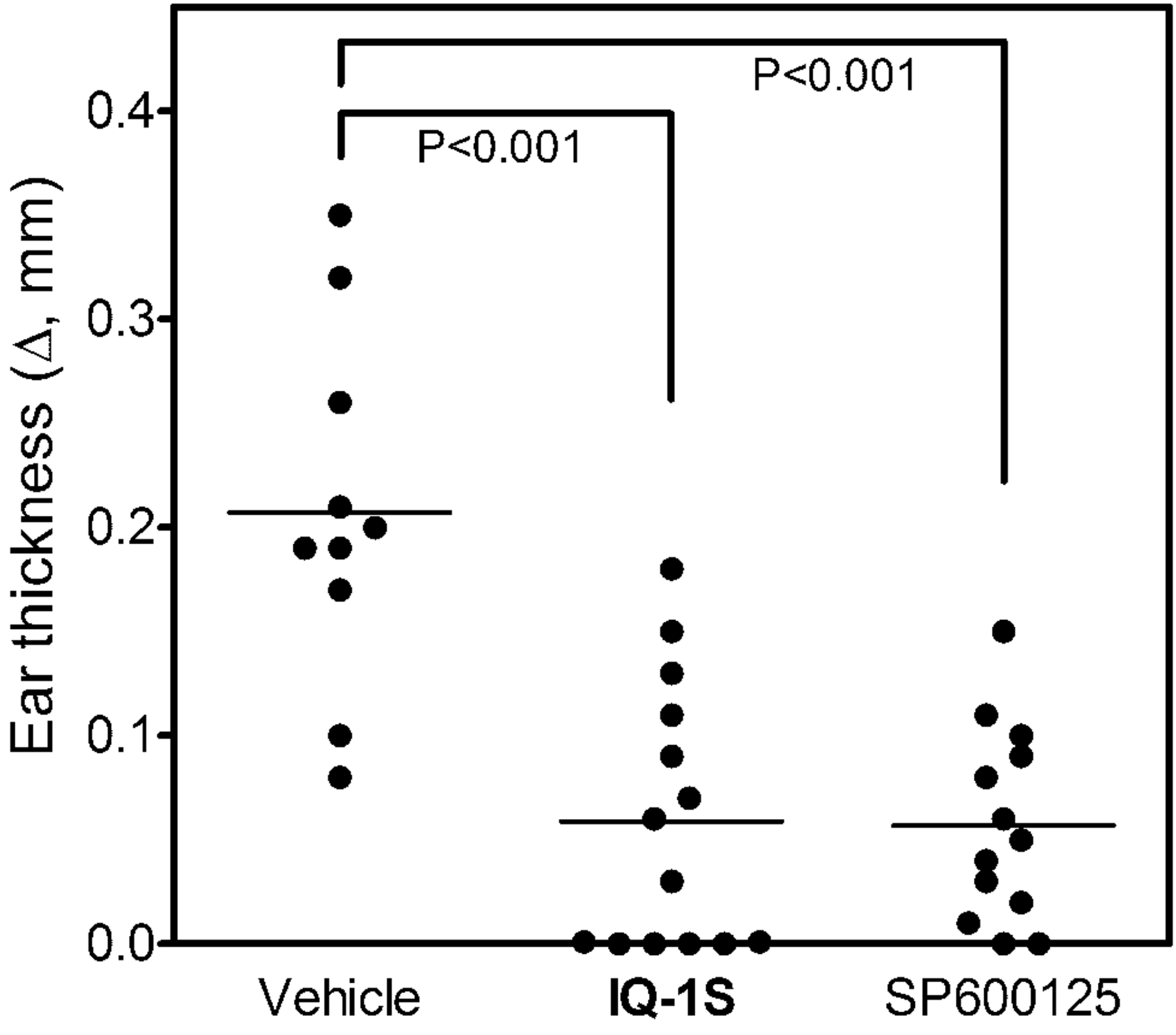
P<0.001
P<0.001
0.4
0.3
0.2
0.1
0.0
Ear thickness (Δ, mm)
Vehicle
IQ-1S
SP600125